JAHRBUCH DER GEOLOGISCHEN BUNDESANSTALT

Jb. Geol. B.-A. | ISSN 0016–7800 | Band 142 | Heft 1 | S. 73–93 | Wien, Mai 2000

Petrotectonics of an Austroalpine Eclogite-Bearing Complex (Sieggraben, Eastern Alps) and U-Pb Dating of Exhumation

MARIÁN PUTIŠ, SERGEY P. KORIKOVSKY & YURI D. PUSHKAREV*)

14 Text-Figures and 8 Tables

Burgenland
Eastern Alps
Crystalline Basement
Sieggraben Complex
Exhumation
Eclogites
Mylonites

Österreichische Karte 1 : 50 000
Blätter 106, 107

Inhalt

Petrotektonik des Eklogit führenden Sieggrabener Komplexes und U-Pb-Daten zu seiner Exhumation

Zusammenfassung

Die oberostalpine Sieggrabener Einheit am Südostrand der Alpen gilt als subduziertes und später exhumiertes Krustenfragment. Die frühalpine Subduktion (DR1-Stadium, P = 14–15 kbar, T ca. 700°C) und die folgende kollisionsbedingte Zerrung sind durch unterkretazische Alter von 137±1–109,3±1 Ma (^{40}Ar–^{39}Ar; Amphibole aus Amphiboliten [DALLMEYER et al., 1992, 1996]) oder 103±14 Ma (U-Pb; Zirkon und Monazit aus Granitgneisen [PUTIŠ et al., 1994, und diese Arbeit]) belegt.

Die frühalpine, kollisionsunterstützte Exhumation (DR2-Stadium) wurde durch eine mittel- bis oberkrustale Störungszone im Liegenden der Sieggrabener Einheit unterstützt. Der Prozess wurde erleichtert durch dynamische Aufweichung in Pyroxen- und Zoisit-Aggregaten in tiefkrustalen Niveaus. Dynamische Rekristallisation von Feldspäten und Amphibolen und Migrationsrekristallisation von Bänderquarz in Granitgneisen und Bänderamphiboliten deuten auf einen Übergang zu mittelkrustaler Rheologie während einer SSE-vergenten Scherung und Hebung der Sieggrabener Einheit.

Gefügestudien mit U-Tisch zeigen deutlich eine bevorzugte Orientierung von Omphazit 1 und Zoisit 1 in Lineation und Schieferung als Folge metamorphen Wachstums (DR1). Andere Mineralien wie Omphazit 2, Zoisit 2, Plagioklas, Kalifeldspat, Quarz und Kalzit zeigen Anzeichen duktiler Deformation. Eine {010}[001]-Translation fand in Plagioklasen bei mittleren Temperaturen (DR2) statt. Quarzgefüge zeigen das bei mittleren Temperaturen dominierende <a>-Prisma und in der höher temperierten Phase des DR2-Stadiums rhombische Translation. Die basale <a>-Translation wirkte in Quarz während der niedriger temperierten Phase des DR2-Stadiums. Niedrig temperierte e-Lamellen in Calzit (DR2) beweisen mechanische Verzwillingung als hauptsächlichen Deformationsmechanismus, dynamische Rekristallisation in den C-Ebenen ist zu vernachlässigen.

*) Authors' addresses: MARIÁN PUTIŠ: Comenius University, Faculty of Natural Sciences, Department of Mineralogy and Petrology, Mlynská dolina, SK-84215 Bratislava, Slovak Republic, Fax: +421-7-60296293, E-mail: putis@fns.uniba.sk; SERGEY P. KORIKOVSKY: Russian Academy of Sciences, Institute of Geology of Ore Deposits, Petrography, Mineralogy and Geochemistry, Staromonetny per. 35, 109017 Moscow, Russian Federation, Fax: +7-095-2302179. E-mail: korik@msk.ru; YURI D. PUSHKAREV: Russian Academy of Sciences, Institute of Precambrian Geology and Geochronology, Makarova Emb. 2, 199034 St. Petersburg, Russian Federation, Fax: +7-812-218401, E-mail: lev@ad.iggp.raas.spb.ru.

Reaktionsmikrostrukturen (DR2) von Eklogiten, Amphiboliten, Marmoren und Gneisen reflektieren eine beinahe isothermale Dekompression zumindest während der ersten Periode der Hebung: DR2-1-HP/MP-HT-Stadium: T = 730–770°C, P <12 kbar, gefolgt vom DR2-2-MP/LP-MT-Stadium: T = 650–550°C, P <8 kbar.

Die mittelostalpine Sieggrabener Einheit scheint innerhalb eines ausgedünnten passiven Kontinentalrandes des Meliata-Hallstatt-Ozeans an der Jura-Kreide-Grenze subduziert worden zu sein. Die obduktionsartige Freilegung (DR2, 137±1–109,3±1 Ma bzw. 103±14 Ma) entlang einer Abscherungszone wurde später zu einer Überschiebung über das Unterostalpin, die gut belegt ist durch Datierungen des alpinen Metamorphosehöhepunktes (T 500°C bei P 10 kbar [KORIKOVSKY et al., 1998]) um 109±18 Ma (Zirkone aus dem Wiesmather Orthogneis, unterostalpine Wechseleinheit [KORIKOVSKY et al., 1998) im überschobenen Unterostalpin.

Das oberkretazisch-untertertiäre Zerrungsereignis (DR3, seit ca. 85 Ma, K-Ar-Daten) folgte der Schließung des Penninischen Ozeans und bewirkte die Freilegung begrabener unterostalpiner und penninischer Struktureinheiten. Dieses Ereignis bzw. eine WSW-vergente Dehnungs-Scherung wurde hauptsächlich durch die niedrigtemperierte Quarzrheologie kontrolliert. Obwohl diese Scherung im Unterostalpin penetrativ wirkt, wurde nur die Basis der Sieggrabener Einheit reaktiviert.

Abstract

The Austro-Alpine (AA) eclogite-bearing complex of the Sieggraben structural unit (= SSU) occurs at the southeastern margin of the Eastern Alps. It is inferred to be a subducted and then exhumed basement fragment. Early Alpine subduction (DR1, HP/HT event: P = 14–15 kbar, at T ca. 700°C) and the following collision-driven extensional (DR2) event are constrained by the dominated Early Cretaceous isotope ages of 137±1–109.3±1 Ma (^{40}Ar–^{39}Ar plateau data on amphiboles from amphibolites [DALLMEYER et al., 1992, 1996]), or 103±14 Ma (U-Pb-lower discordia intercept using zircon and monazite from granite-gneisses [PUTIŠ et al., 1994, and this paper]).

The Early Alpine collision-driven exhumation (DR2) was enhanced by a mid- to upper-crustal master detachment fault located in the footwall of the SSU. The exhumation process was firstly accommodated by dynamic strain softening in pyroxene (omphacite) and zoisite aggregates at the lower-crustal level. Dynamic recrystallization of feldspars, amphibole and migration recrystallization of quartz into ribbons in granite-gneisses and layered amphibolites indicate a transition to mid-crustal rheology during a top-to-the SSE hanging wall extensional shearing (DR2) and uplift of the SSU.

Textural U-stage microscope patterns document a pronounced preferred orientation of omphacite 1 and zoisite 1 in lineation and foliation due to oriented metamorphic (DR1) growth. Other minerals like omphacite 2, zoisite 2, plagioclase, potassium feldspar, quartz and calcite bear the features of ductile deformation by micromechanisms of dislocation flow. {010}[001] glide operated in plagioclase at medium temperatures (DR2). Patterns of quartz reveal dominated medium-temperature prism <a>, less rhomb glide during the higher temperature period of the DR2 stage. Calcite low-temperature (DR2) e-lamellae indicate mechanical twinning as the main deformation micromechanism, with negligible contrubution of dynamic recrystallization in the C-planes.

Reaction microstructures (DR2) of eclogites, amphibolites, marbles and gneisses reflect almost isothermal decompression at least during the first period of the uplift: DR2-1-HP/MP-HT stage: T = 730–770°C, P <12 kbar, followed by DR2-2-MP/LP-MT stage: T = 650–550°C, P <8 kbar.

The Middle AA Sieggraben structural unit (SSU) seems to have been subducted within a thinned passive continental margin of the Meliata-Hallstatt Ocean approximately at the Jurassic-Cretaceous boundary period. The obduction-like exhumation (DR2, 137±1–109.3±1 Ma or 103±14 Ma, respectively) along a master detachment fault transformed into the thrust over the LAA structural complex. It is well constrained by dating of Alpine metamorphism climax conditions (T 500°C at P 10 kbar [KORIKOVSKY et al., 1998]) at 109±18 Ma (U-Pb-lower discordia intercept using zircon from the LAA Wechsel structural unit Wiesmath orthogneiss [KORIKOVSKY et al., 1998]) in the buried LAA structural complex.

The Late Cretaceous–Early Tertiary collision-related extensional event (DR3, since ca. 85 Ma, K-Ar data) thus followed the closure of the Penninic Ocean. It enhanced the exhumation of buried LAA (and Pennine) structural complexes in some domes and tectonic windows. This event, or a top-to-the WSW extensional shearing was mainly controlled by the low-T quartz rheology. Although it is penetrative for the LAA structural complex, only the basis of the SSU was reactivated.

1. Introduction and Geological Setting

The Austro-Alpine (AA) Sieggraben eclogite-bearing structural unit is located at the south-eastern margin of the Eastern Alps or within the internal part of the Alpine orogenic belt (Text-Fig. 1, 2). TOLLMANN (1977) ascribed it to the Middle Austro-Alpine (MAA) structural complex.

The paper contributes to regional problems of progradation of the Cretaceous orogeny in alpidic internides. Two collision-driven extensional events (DR2 and DR3 deformation-recrystallization stages) followed after the closing of the two distinctive oceans: the Meliata-Hallstatt (KOZUR, 1991; PLAŠIENKA, 1991; PUTIŠ, 1991; NEUBAUER, 1994) and the Pennine one. An inferred record of those events was tried to be distinguished in the area of the villages Sieggraben and Schwarzenbach (Text-Fig. 2) using a methodically combined geological-structural, textural, petrological and geochronological approach.

The paper analyses deformation-recrystallization evolution of the deep-seated mylonites within the detachment shear zones developed during the DR2 and DR3 events (Text-Fig. 3) following an A-type subduction (DR1). The reconstructed P-T path (Text-Fig. 4) of eclogite and amphibolite facies rocks is closely related to their deformation path and both document the existence of a deep-crustal detachment zone responsible for the exhumation of the Sieggraben structural unit (SSU).

Concerning the previous results and views, the MAA basement, including the Sieggraben structural unit (SSU), is inferred to have formed as a part of the Koriden terrane (FRISCH & NEUBAUER, 1989; NEUBAUER & FRISCH, 1993). It represents an accretional wedge, derived from the flysch-like sediments and ocean fragments near a trench located on the upper (northern) Variscan plate (MATTE, 1986, 1991).

The southern parts of the AA domain, along with the southern parts of the central Western Carpathians basement complexes represent a Paleotethyan remnant (STAMPFLI, 1996; PUTIŠ & GRECULA, in PLAŠIENKA et al., 1997) incorporated into a passive continental margin of the Triassic-Jurassic Meliata-Hallstatt Ocean (KOZUR, 1991; PLAŠIENKA, 1991; PUTIŠ, 1991; NEUBAUER, 1994).

The MAA (Koriden) basement of the Saualpe and Koralpe of the Eastern Alps comprises perhaps both pre-Alpine (693 Ma, Sm-Nd, Grt-WR [MANBY & THIEDIG, 1988; MANBY et al., 1989]) and Alpine (275±18 Ma, Sm-Nd, Pl-Cpx-WR

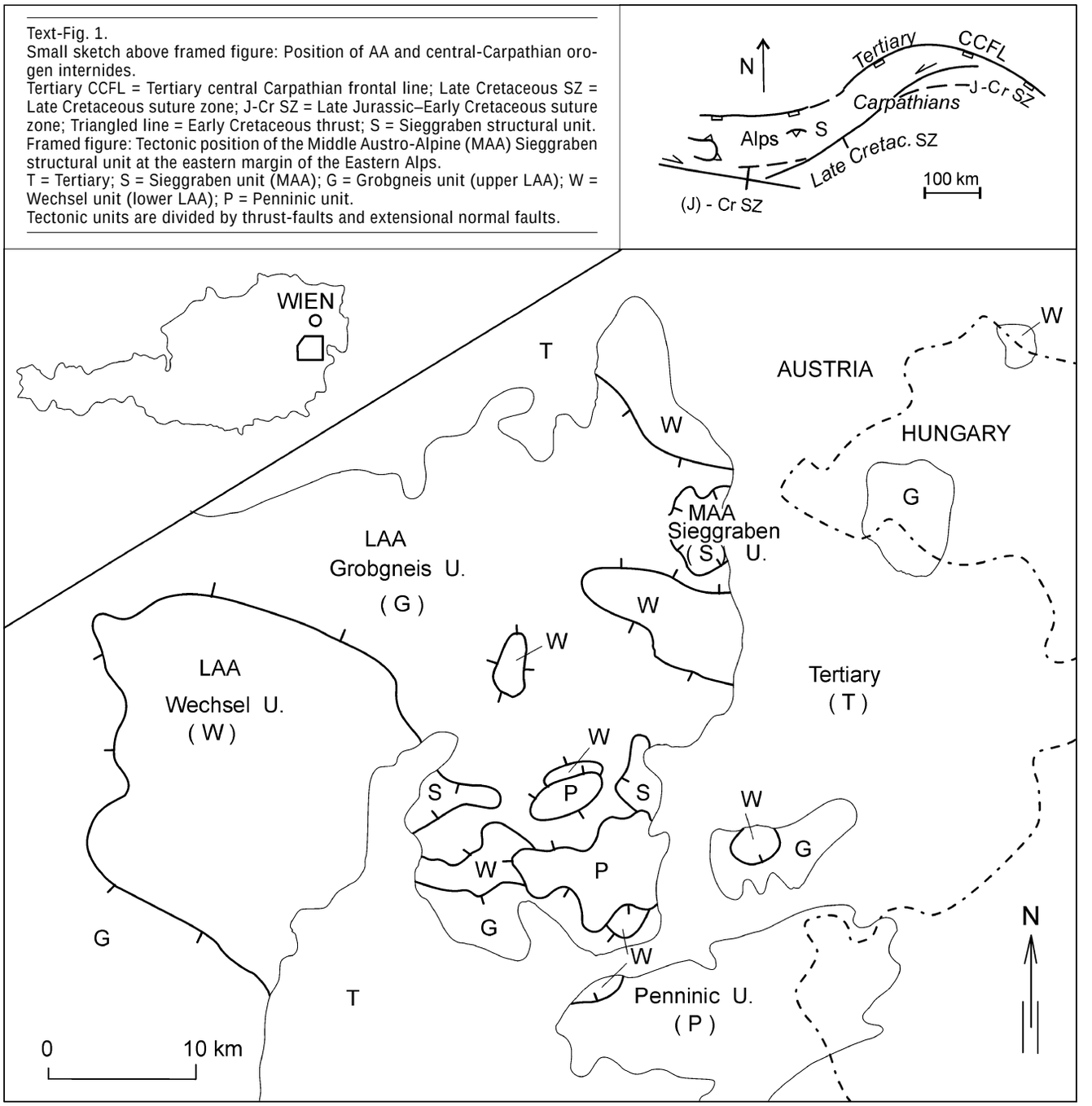

Text-Fig. 1.
Small sketch above framed figure: Position of AA and central-Carpathian orogen internides.
Tertiary CCFL = Tertiary central Carpathian frontal line; Late Cretaceous SZ = Late Cretaceous suture zone; J-Cr SZ = Late Jurassic–Early Cretaceous suture zone; Triangled line = Early Cretaceous thrust; S = Sieggraben structural unit.
Framed figure: Tectonic position of the Middle Austro-Alpine (MAA) Sieggraben structural unit at the eastern margin of the Eastern Alps.
T = Tertiary; S = Sieggraben unit (MAA); G = Grobgneis unit (upper LAA); W = Wechsel unit (lower LAA); P = Penninic unit.
Tectonic units are divided by thrust-faults and extensional normal faults.

isochrons from the core of an eclogite body, and Grt-WR Sm-Nd age of 93±15 Ma from an eclogitic part of the same outcrop [THÖNI & JAGOUTZ, 1992, 1993]) eclogites. The latter apparently resemble those of the Sieggraben unit. The MAA structural complex comprises metapelites (gneisses, micaschists), metabasites (eclogites, amphibolites, metagabbros), metaultramafics (serpentinites), metagranitoids (leucocrate metagranites, metapegmatites) and less metacarbonates, comparable with the lithological sequence of the MAA Sieggraben structural unit (KÜMEL, 1935; PUTIŠ, 1992a) (Text-Fig. 2).

The Early Alpine evolution of the southeastern edge of the AA basement and cover complexes is related to the evolution of a continental margin adjoining to the northern side of the Meliata-Hallstatt Ocean (Text-Fig. 3). The same is valid for the Veporic and Gemeric structural units of the central Western Carpathians located to the north of the Meliata unit suture zone (or the Rožňava line).

The southern parts of the central Western Carpathians basement and cover complexes, which are nearly in the "AA" position, yield radiometric ages of 278–216 Ma for the Early Alpine continental rifting phase ([KOTOV et al., 1996] U-Pb data). Similarly, Rb-Sr Permian ages 270–240 Ma (FRANK et al., 1987; DALLMEYER et al., 1992) and a Sm-Nd Pl-Cpx-WR isochron (275±18 Ma) of a gabbro (THÖNI & JAGOUTZ, 1992) in the MAA Koriden Complex appear to be related to the first stage of the Early Alpine extension leading to the development of the early Tethys in the Permian–Triassic period at the southern margin of the AA realm.

The Late Cretaceous–Early Tertiary dome structures at the eastern margin of the Eastern Alps coincide quite well with the formation of the Vepor dome/core structure at the SE margin of the neighbouring central Western Carpathians (PLAŠIENKA & PUTIŠ, 1993; PLAŠIENKA, 1993; PUTIŠ, 1992b, 1994). Tectonic linkage of these domains has already been proposed (PUTIŠ, 1991; NEUBAUER, 1994).

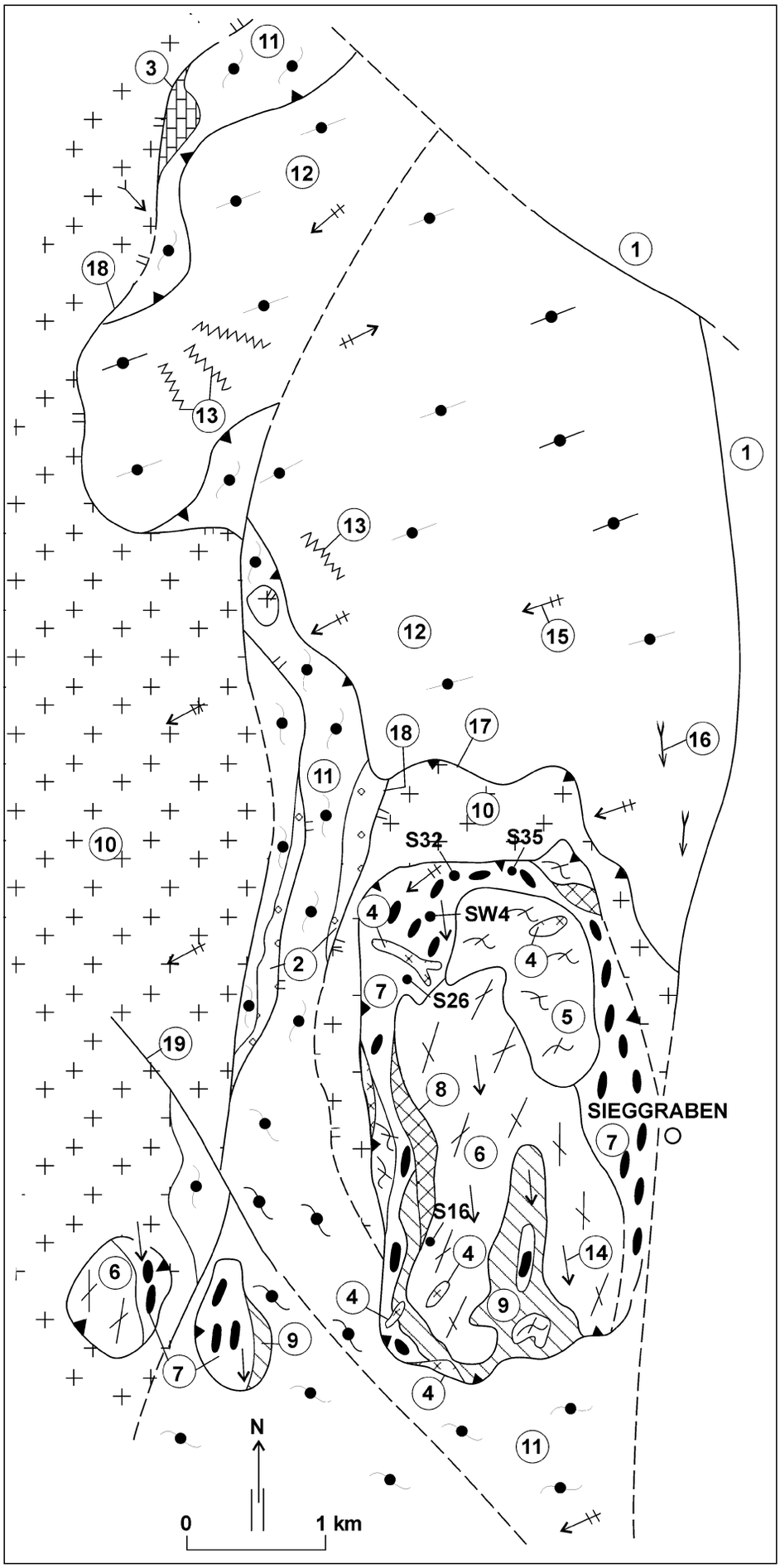

Text-Fig. 2.
Geological-tectonic sketch-map of the Middle and Lower Austro-Alpine basement and cover complexes in the Sieggraben area (PUTIŠ, 1992a).
1 = Tertiary; 2–3 = Permo-Mesozoic cover: 2 = Permo-Scythian metasandstones and metaconglomerates, 3 = mid-Triassic metacarbonates; 4 = granite, pegmatite; 5 = Micaschist Complex; 6 = Gneiss Complex; 7–9 = Eclogite-amphibolite (= 7) Serpentinite (= 8) Marble (= 9) Complex; 10–11 = LAA Grobgneiss unit: 10 = mylonitic granite-gneiss (Grobgneis), 11 = paragneiss; 12 = LAA Wechsel-like unit (phyllites, greenschists, porphyroids); 13 = Qtz vein; 14 = medium-T lineation (DR2); 15 = low-T lineation (DR3); 16 = crenulation lineation; 17 = normal fault (late DR3); 18 = internal thrust (early DR3) of a structural unit; 19 = fault. Lineations and foliations are subhorizontal.
U-Pb dating (PUTIS et al., 1994) was performed on granitic veins (4) cca. 2 km northwest (sample SG1) and southwest (sample SW2) of Sieggraben.
S35, SW4, S32, S26, S16 = location of petrological samples (from Tab. 1–7).

The Austro-Alpine Nappe Complex represents a thick-skinned fold and thrust belt interpreted to have comprised the upper continental plate during the Tertiary collision of the European foreland/Penninic continental crust and Adriatic microplate (NEUBAUER & VON RAUMER, 1993). However, earlier, during the Early Cretaceous orogeny (after the closing of the Meliata-Hallstatt Ocean), the SSU participated as a part of the lower-plate passive margin (NEUBAUER, 1994; DALLMEYER et al., 1996).

Mineral ages, decreasing from the hanging wall to footwall structural units (UAA: 140–125 Ma, MAA: 136–85 Ma, LAA: 125–70 Ma) according to the $^{40}Ar/^{39}Ar$ method (DALLMEYER et al., 1992, 1996) are interpreted to indicate a tectonic pattern, which reflects in the Cretaceous a long-term collision footwall propagation of a master fault (DALLMEYER et al., 1992; NEUBAUER et al., 1992; NEUBAUER, 1994). This pattern, however, does not comprise the complexity of the exhumation process of the MAA and LAA structural units in the studied region.

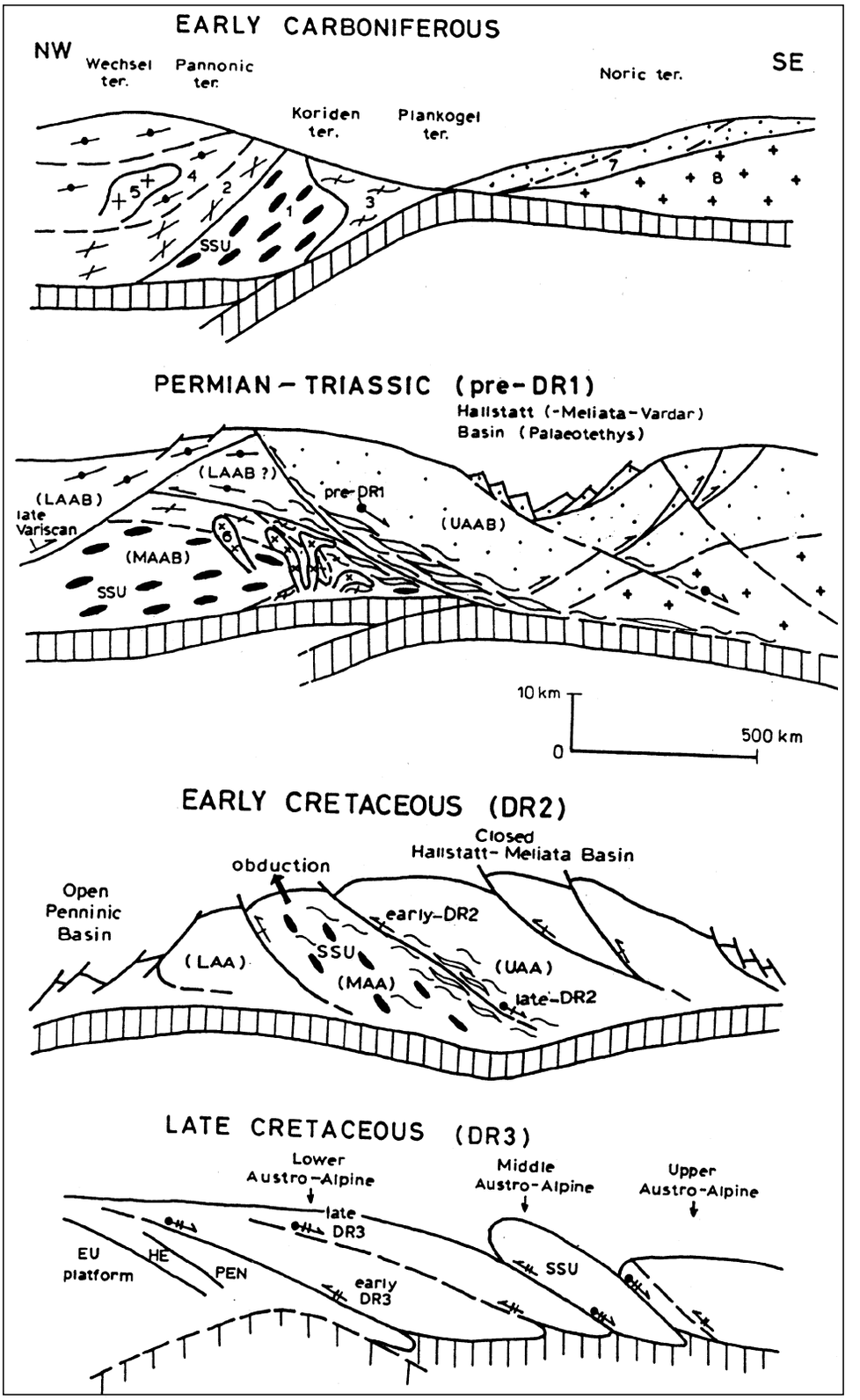

Text-Fig. 3.
Evolution of the MAA Sieggraben structural unit (SSU).

MAAB = Middle Austro-Alpine basement
1 = eclogites, amphibolites (pre-Apine metabasites, metaultramafics and marbles, originally); 2 = Ky-Sil gneisses (Pre-Alpine metapelites, originally); 3 = micaschist (pre-Alpine metapelites, originally); 6 = orthogneisses (granites and pegmatites, originally).

LAAB = Lower Austro-Alpine basement
4 = micaschist gneisses to phyllites (Early Palaeozoic?); 5 = grobgneis-type orthogneisses (Variscan porphyric granites, originally), UAAB = Upper AA basement; 7 = low-grade metamorphic rocks (Early Palaeozoic); 8 = Cadomian(?) unknown basement rocks, ter = terrane, PEN = Pennine, HE = Helvetic, EU = European.

Radiometric data suggest an Early Cretaceous exhumation of amphibolized eclogites in the time interval between 137±1 and 109.3±1 Ma (^{40}Ar–^{39}Ar plateau data on amphibole [DALLMEYER et al., 1992, 1996]). An age of 103±14 Ma was found in a granite-gneiss (U-Pb-lower discordia intercept on Zr and Mnz [PUTIŠ et al., 1994; PUTIŠ & KORIKOVSKY, 1993, 1995]) cutting the Sieggraben metabasite-marble complex.

THÖNI & JAGOUTZ (1992, 1993) dated gabbroic rocks of Permian age and therefore proved the existence of Alpine eclogites within the MAA basement. They suggested the age of the HP event in a time interval of ca. 150–100 Ma. However, they found out rejuvenation of all applied isotope systems within the hydrated shear zones that is also reflected by a disequilibrium in studied isotopic systems (Sm-Nd, Rb-Sr and K-Ar) of the major mineral components in eclogites: Grt, Cpx1-3, Zo/Ep, Phe, Am and Rt. The Sm-Nd data for WR, Grt, Cpx1-3 and Am of the eclogite show clear isotopic disequilibrium: WR and Grt define an isochron age of 93±15 Ma (the Rb-Sr age for this pair is 100 Ma), WR-Cpx3 (Om) an age of 151 Ma (the Rb-Sr age for this data pair is 140 Ma). The Sm-Nd isochron of 95,5±9,5 for Grt, Cpx3 and Phe for eclogite is identical with the 95±1 Ma Rb-Sr age of Phe (Koralpe – Bärofen).

2. Methodical Approach

The methodical approach is directed to some open questions concerning the polyphase evolution of the Sieggraben structural unit (SSU) within the AA internides.

These are mainly:

– The mode of emplacement and kinematics of an eclogite-bearing nappe during the Cretaceous orogeny.
– Conditions of deformation-recrystallization (DR) stages.

Text-Fig. 4.
Estimated P-T path of the Sieggraben eclogite-bearing structural unit.
Further explanation in text.

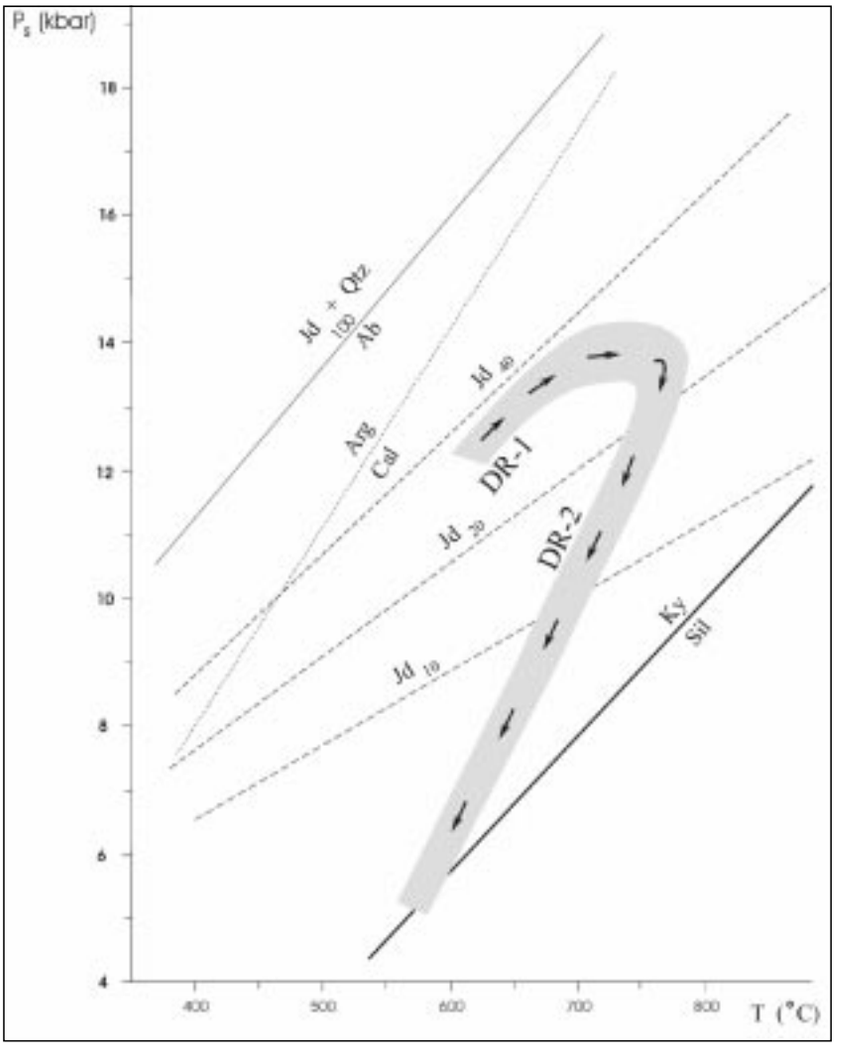

– Rheological behaviour and textural patterns of some rock-forming minerals.
– The age of DR events.

The mode of emplacement was solved in the scale of the new geological map 1 : 10.000 in the area of the villages Sieggraben and Schwarzenbach (an Austrian Geological Survey mapping project [PUTIŠ, 1992a, Text-Fig. 2]) as well as by application of structural-geological techniques (PUTIŠ, 1995).

Deformation-recrystallization relationships were firstly studied in detail from oriented thin-sections under a polarized microscope. The Petrographical description of the different DR stages is documented by macro- and micro-photographs (Text-Fig. 8–10).

All rock-forming minerals were analyzed in polished sections using a CAMSCAN electron microprobe equipped with a LINK H.E.D.A. system at Moscow State University. Some representative microprobe analyses of key minerals are summarized in Tab. 1–7 and their chemical compositions are depicted in Text-Fig. 5–7. Fe^{2+} and Fe^{3+} were computed with a computer program assuming stoichiometry and charge balance, taking into account recommendations of SCHUMACHER (1991).

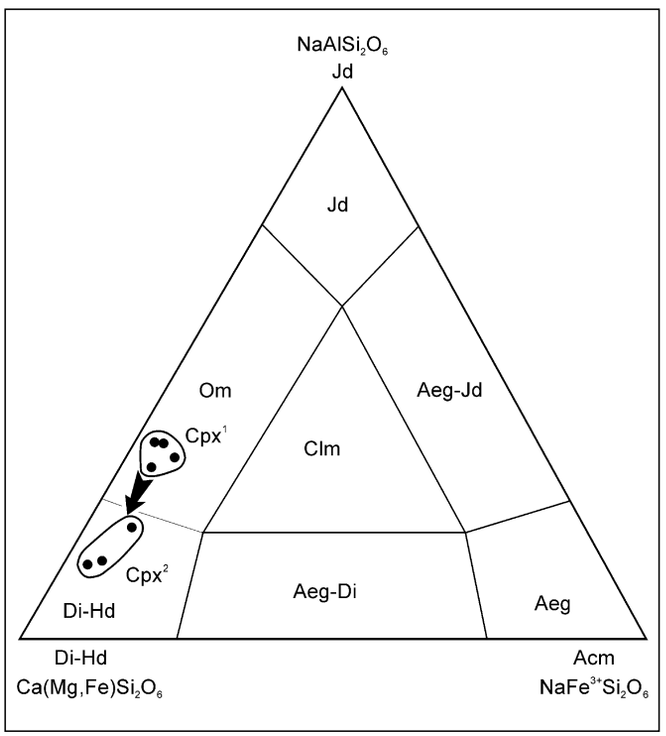

Text-Fig. 5.
Composition diagram of pyroxenes in eclogite.
Cpx1 (Om, S35b, SW4/14, SW4/16, Tab. 1), DR1 HP/HT event. Cpx2 (Di, S32b, S26c, Tab. 4, 5), DR2 MP/HT event.

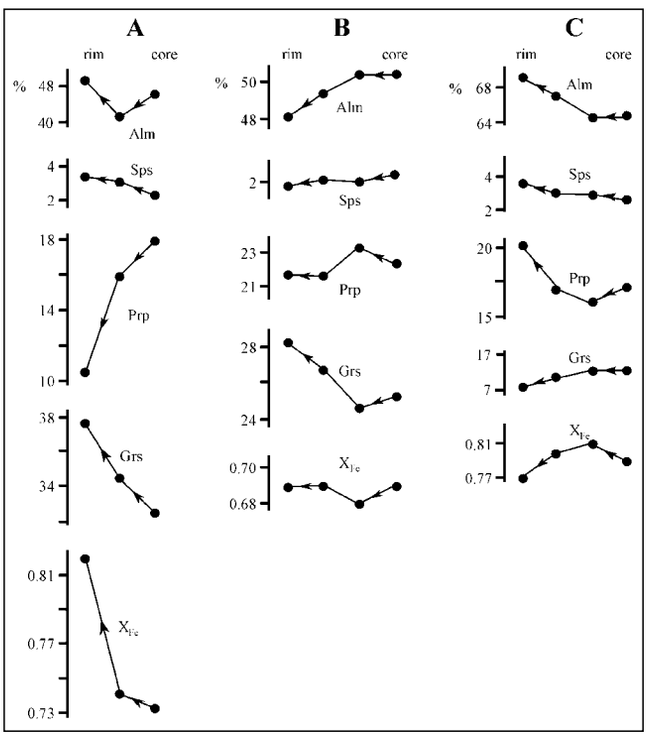

Text-Fig. 6.
Prograde and retrograde compositional zoning in garnets.
Left (S32b) and middle (S26c) in Grt amphibolite (Tab. 3, 4), right in paragneiss (S16b, Tab. 7).

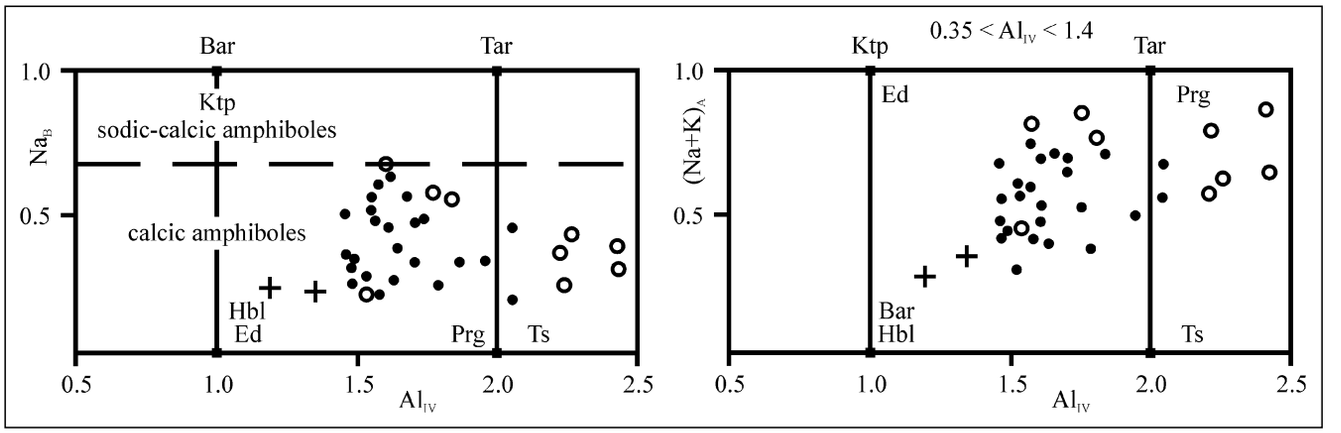

Text-Fig. 7.
Composition diagram of amphiboles in eclogites, amphibolites and marbles.
Black points = Hbl1 (DR1) in eclogites (S35b, SW4/14, SW4/16) and amphibolites (S32b, S26c), Tab. 4, 5, 6; circles = Hbl2 (DR2) in eclogites and amphibolites around Grt in contact with Cpx1 (SW4/16) or Hbl1 (S26c/2), Tab. 6; crosses = Hbl2 (DR2) around Cpx in impure marbles.

Andradite end-members (Fe^{3+} content) in garnets are very low (0–3 %) and therefore for simplicity we calculated garnet analyses for 4 end-members: Alm, Sps, Prp and Grs.

For obtaining PT-estimates we used equilibrial mineral assemblages of the DR1 and DR2 stages in Grt-Cpx thermometers of PATTISON & NEWTON (1989), KROGH (1988) and POWELL (1985); Grt-Hbl thermometers of GRAHAM & POWELL (1984), BLUNDY & HOLLAND (1990) and HOLLAND & BLUNDY (1994); Grt-Cpx-Pl-Qtz barometer of ECKERT et al. (1991); Grt-Hbl-Pl-Qtz barometer of KOHN & SPEAR (1989) for those associations with Na in Hbl less 0.6 f.u., Grt-Pl-aluminium silicate-Qtz barometer of MCKENNA & HODGES (1988) and Grt-Px-Pl-Qtz barometer of PERKINS & NEWTON (1981).

P-T parameters (Text-Fig. 4) were reconstructed using the mineral succession relationships. The distinguishing DR1, DR2, and DR3 stages were performed on the basis of observed mineral and microstructural changes. The climax conditions of the estimated PT-path correspond with Jd38-isopleth for Cpx-Ab-Qtz association (HOLLAND, 1980).

Sample	S35b			SW4/14	SW4/16	S35b	SW4/14	SW4/16
Phase	Cpx1 (Om large grains)					Cpx2 from Cpx2-Pl symplectite		
SiO_2	55.29	55.72	54.99	51.99	51.90	54.20	51.74	50.76
TiO_2	0.19	0.23	0.19	0.17	0.24	0.25	0.29	0.21
Al_2O_3	9.52	9.47	9.17	8.52	8.52	7.34	5.61	7.26
FeO	6.21	6.06	4.98	7.60	7.58	5.58	8.35	9.28
MnO	-	-	-	0.15	0.09	-	0.10	0.02
MgO	8.48	8.60	8.11	7.75	7.87	9.90	9.84	10.99
CaO	13.68	13.47	14.56	14.16	13.94	16.64	17.17	19.01
Na_2O	5.86	6.06	6.23	5.53	5.70	4.40	3.67	2.35
K_2O	-	-	-	0.06	0.03	-	-	0.08
Fe_2O_3*	1.11	1.49	3.14	3.53	4.20	2.95	3.51	4.11
Total	100.34	101.10	100.37	99.46	100.07	101.26	100.27	100.07
Si	1.99	1.99	1.98	1.96	1.95	1.95	1.96	1.95
Al_{IV}	0.01	0.01	0.02	0.04	0.05	0.05	0.04	0.05
Al_{VI}	0.39	0.39	0.37	0.34	0.33	0.21	0.21	0.10
Ti	0.01	0.01	0.01	-	0.01	0.01	0.01	0.01
Fe^{3+}	0.03	0.04	0.09	0.10	0.12	0.08	0.10	0.12
Fe^{2+}	0.19	0.18	0.15	0.14	0.12	0.17	0.16	0.18
Mn	-	-	-	-	-	-	-	-
Mg	0.45	0.46	0.43	0.43	0.44	0.53	0.55	0.63
Ca	0.53	0.51	0.52	0.57	0.56	0.64	0.70	0.78
Na	0.41	0.42	0.43	0.40	0.42	0.31	0.27	0.18
K	-	-	-	-	-	-	-	-
Jd	37.9	37.2	34.9	30.1	28.8	21.9	16.6	5.6
Acm	3.0	4.0	8.6	10.1	12.0	8.0	10.1	12.0
Di	42.3	42.6	41.5	42.8	43.5	51.0	54.2	51.6
Hd	15.5	14.8	12.9	12.9	11.0	14.4	14.7	18.1
Ts	1.3	1.4	2.1	4.1	4.7	4.7	4.4	4.7
X_{Fe}^{2+}	0.30	0.28	0.26	0.25	0.22	0.24	0.23	0.22

Table 1.
Microprobe analyses of primary and secondary Cpx from eclogite (S35b) and eclogite-amphibolite (SW4/14, SW4/16).
*Fe_2O_3 and Fe^{3+} in Cpx calculated from site saturation and charge balance.
Locations: see Text-Fig. 2.

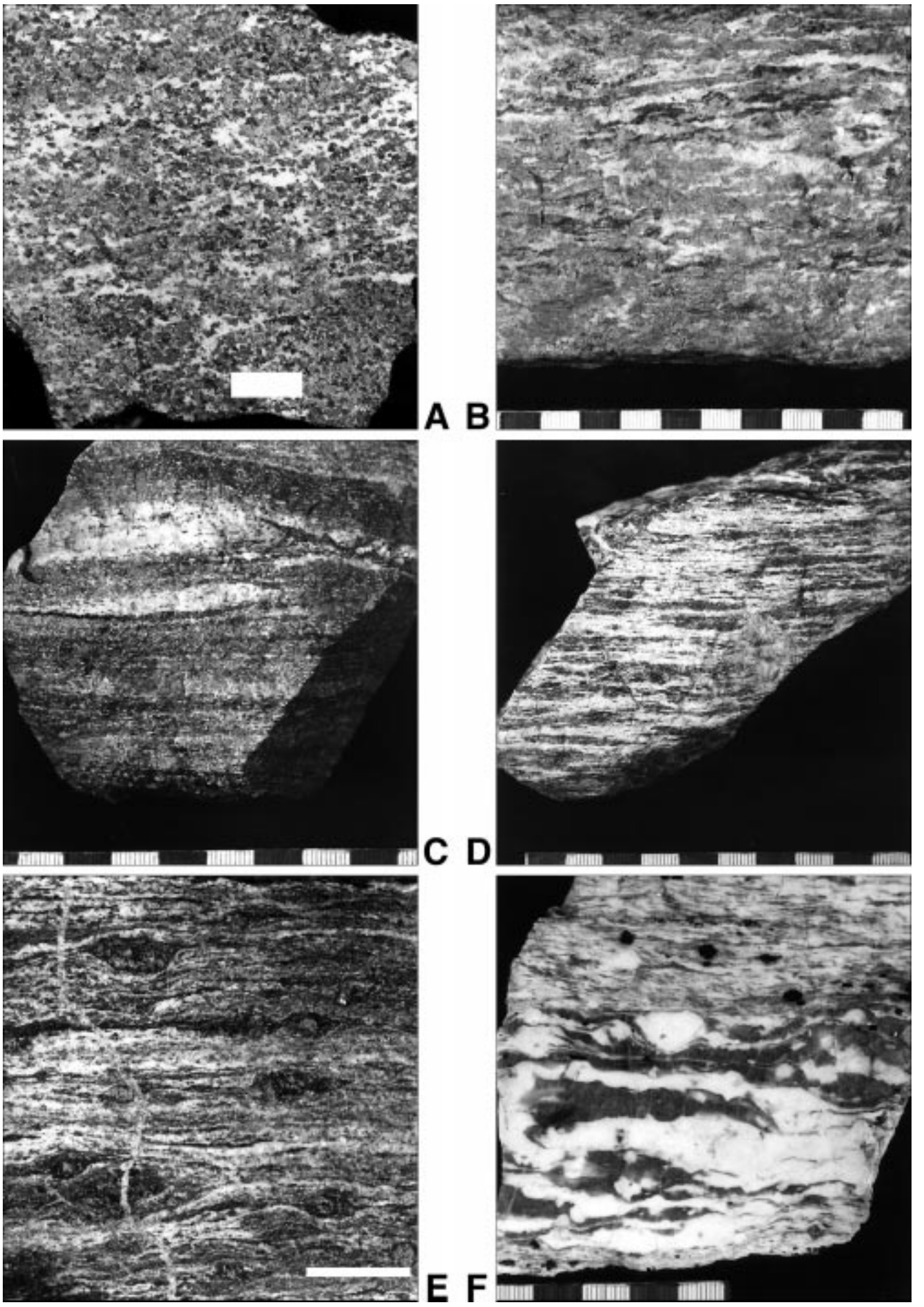
A
B
C
D
E
F

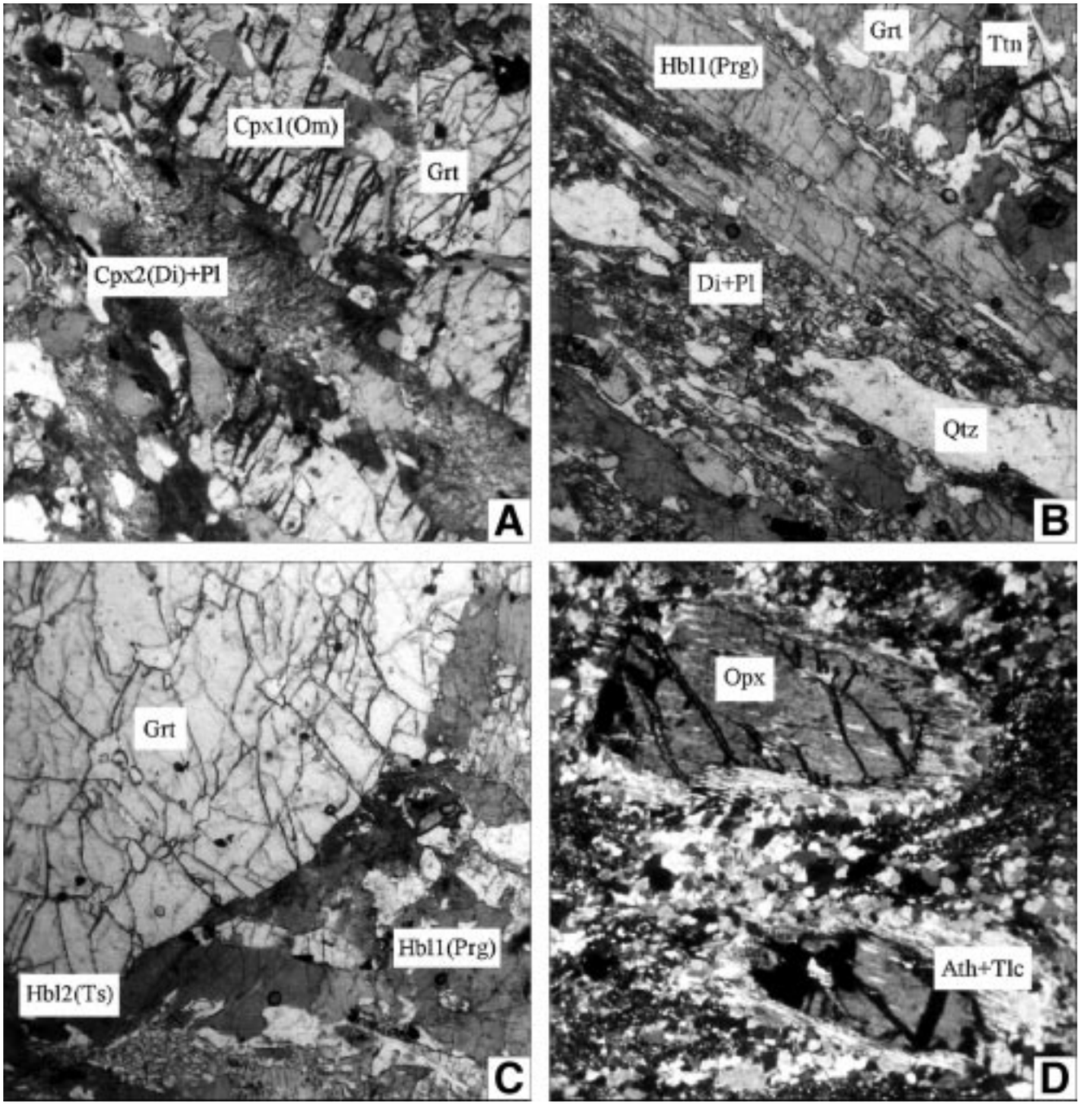

Text-Fig. 9. ▲△▲
Reaction and recrystallization microstructures of eclogites, amphibolites and Opx-Ky-Grt gneisses (MAA Sieggraben unit).

A: Cpx1(Om) + Grt (DR1), Cpx2(Di) + Pl symplectite (DR2), eclogite.
B: A prograde Cpx2(low-Na) + Pl aggregate between Hbl1(Prg) and Qtz (DR2), amphibolite.
C: Hbl2 (Ts-rich) rim between Grt and Hbl1 (Prg), amphibolite (DR2).
D: Ath-Tlc rim around Opx, gneiss mylonite (DR2).

Scale: 1 cm = 0.4 mm.

Text-Fig. 8 (opposite page 80). ◄◁◄
Macrostructures of high- and medium-temperature mylonites (MAA Sieggraben unit).

A: Gabbro-eclogite (DR1).
B: Amphibolized gabbro-eclogite mylonite (DR2).
C: Layered amphibolite (DR2).
D: Amphibolite mylonite (DR2).
E: Impure marble mylonite (DR2).
F: Tourmaline pegmatite mylonite (DR2).

Scale bar = 1 cm.

The relationship of macro- and microstructures to textural (CPO) patterns is also documented by crystallographic preferred orientation patterns of minerals (Text-Fig. 11–12). These were measured by the U-stage microscope technique using omphacite, zoisite, amphibole, plagioclase, quartz and calcite.

The mentioned minerals were utilized as kinematical and deformation mechanism indicators in mylonitic rocks (Text-Fig. 13) that passed through different lithospheric levels during uplift. Their rheological behaviour fits quite well into the suggested P-T-path (Text-Fig. 4).

U-Pb (Text-Fig. 14A, Tab. 8) isotope data enabled us to date the DR2 stage of the eclogite-bearing nappe exhumation. The presented data were measured in the Institute of Precambrian Geology and Geochronology in St. Petersburg (Russian Federation). Zircon, apatite and monazite were extracted from the two (SG1 and SW2) rock samples of the granitic orthogneisses. All measurements were car-

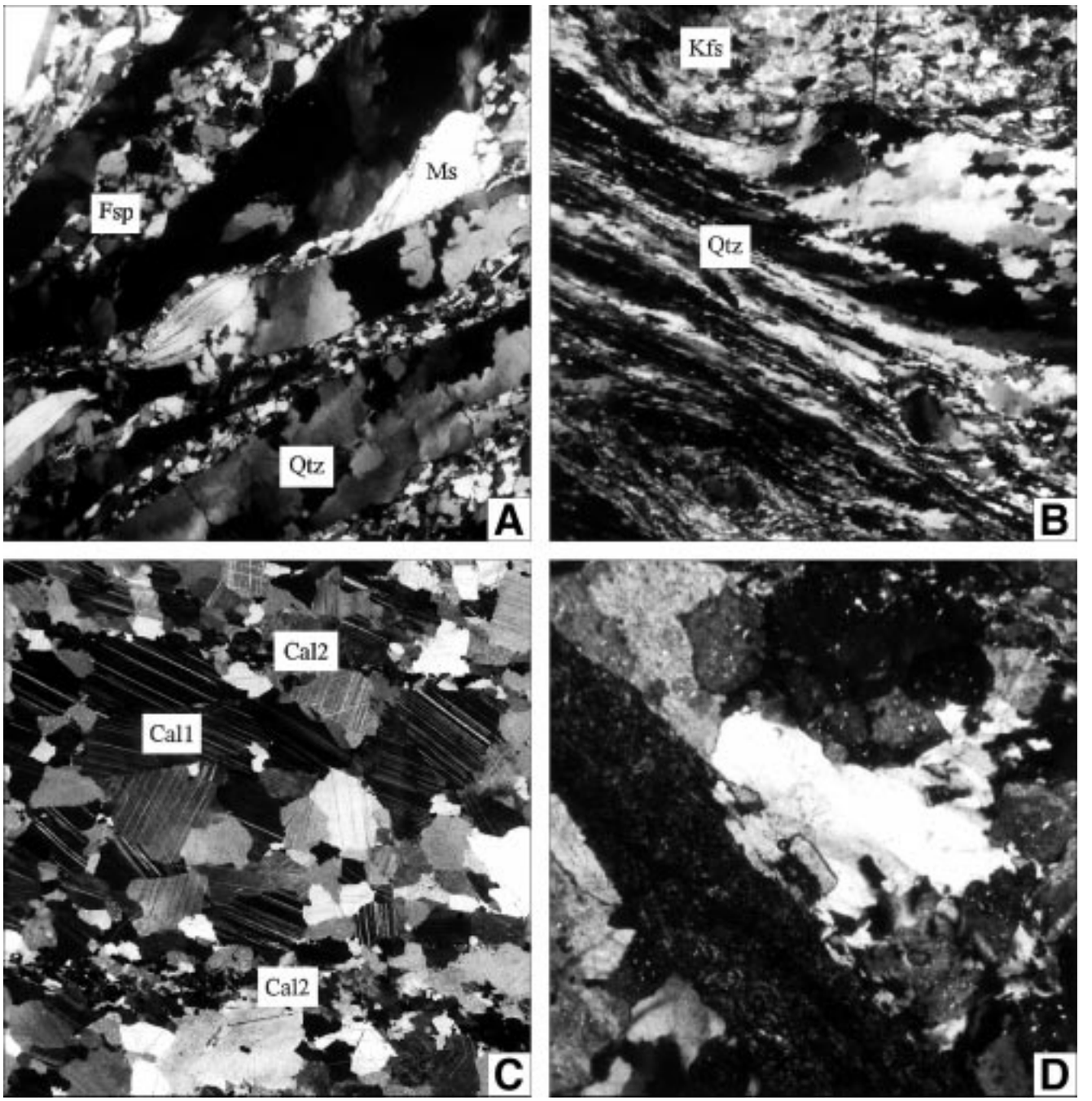

Text-Fig. 10. ▲△▲
Microstructures of medium to low-T mylonites.
A: Qtz ribbons surrounded by dynamicaly recrystallized Fsp matrix (DR2), granitic orthogneiss–mylonite.
B: ductile fibrous Qtz around albitized Kfs porphyroclasts, S-C mylonite of the Grobgneis-type orthogneiss (DR3).
C: flattened Cal grains parallel to e-lamellae (DR2), cut by C-planes with the newly-formed dynamically recrystallized Cal(2) grains, marble.
D: pseudotachylitic matrix, grobgneis-type orthogneiss (DR3?).
Scale: 1 cm = 0.4 mm.

Table 2. ►▷►
Microprobe analyses of Grt from eclogite (S35b). Location: see Text-Fig. 2.

Sample	S35b					
Phase	Grt				Grt	
	core	middle		rim	core	rim
SiO_2	39.15	39.22	39.68	39.75	39.14	39.62
TiO_2	-	-	-	-	0.19	-
Al_2O_3	20.94	21.01	21.48	21.54	21.97	22.54
FeO	24.92	24.18	25.26	24.32	23.18	23.28
MnO	0.95	0.90	0.44	0.40	2.04	0.41
MgO	3.40	3.74	4.29	4.70	3.20	5.01
CaO	10.74	10.71	9.71	9.64	10.48	9.69
Total	100.10	100.39	100.87	100.36	100.21	100.55
Alm	54.5	53.8	55.1	53.5	52.2	51.7
Sps	2.1	2.0	1.0	0.9	4.6	0.9
Prp	13.3	14.4	16.7	18.4	12.9	19.8
Grs	30.1	29.8	27.2	27.2	30.3	27.6
X_{Fe}^{2+}	0.80	0.79	0.77	0.74	0.80	0.72

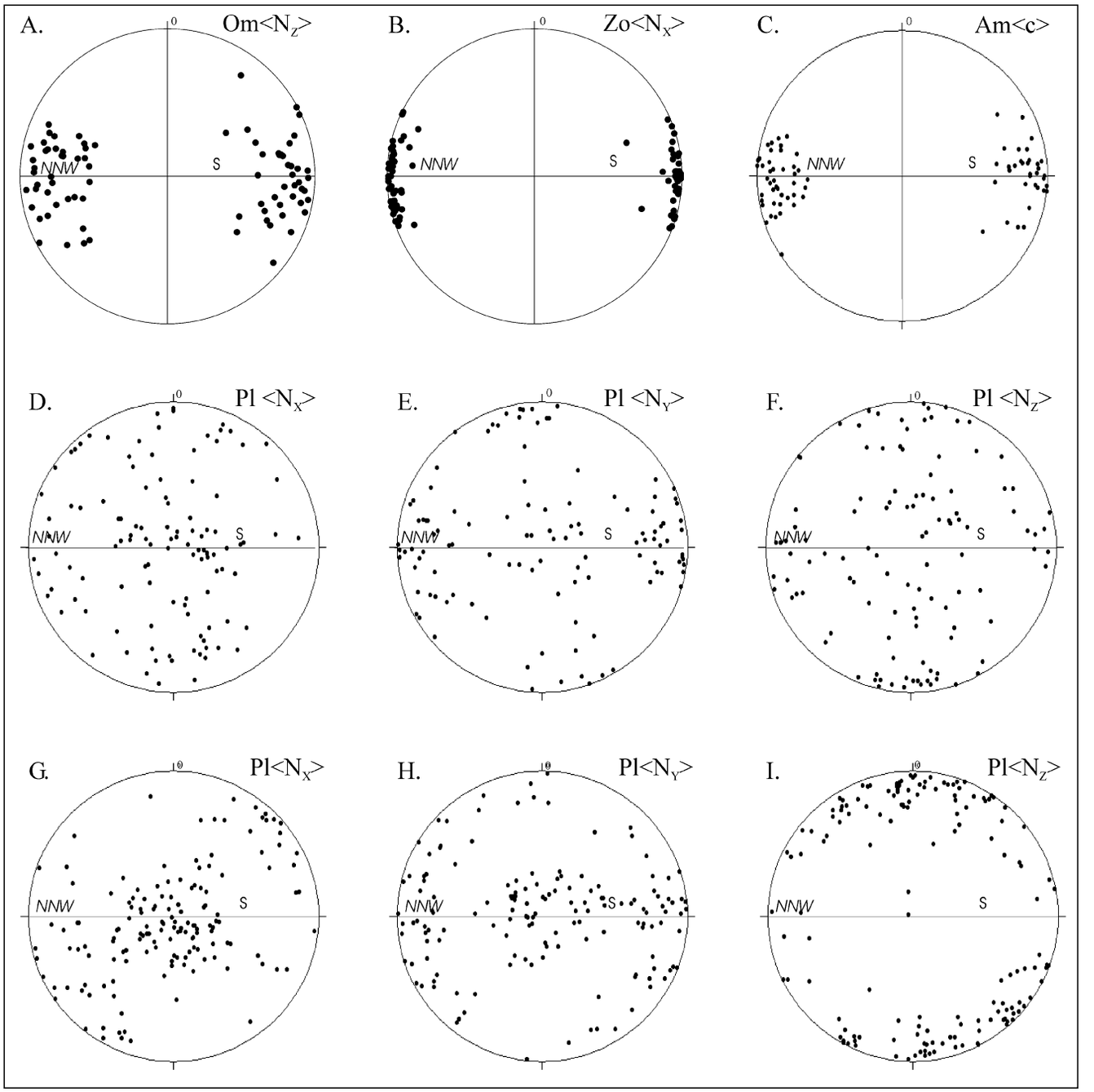

Sample	S26c				S32b		
Phase	Grt				Grt		
	core	middle		rim	core	middle	rim
SiO_2	38.78	38.57	38.89	39.14	40.54	40.43	40.69
TiO_2	0.13	0.13	0.02	0.21	0.22	0.25	0.10
Al_2O_3	21.72	21.98	22.01	21.98	22.19	22.37	22.01
FeO	23.27	23.47	22.79	21.99	20.84	20.25	20.90
MnO	0.96	0.82	0.90	0.81	0.99	1.33	1.44
MgO	5.82	6.07	5.61	5.58	4.37	3.90	2.57
CaO	9.09	8.90	9.69	10.15	11.04	11.76	12.63
Total	99.77	99.85	99.81	99.77	100.20	100.28	100.35
Alm	50.3	50.4	49.4	48.0	47.6	46.4	48.4
Sps	2.1	1.8	2.0	1.8	2.3	3.1	3.4
Prp	22.4	23.2	21.7	21.8	17.8	16.0	10.6
Grs	25.2	24.6	26.9	28.4	32.3	34.5	37.6
X_{Fe}^{2+}	0.69	0.68	0.69	0.69	0.73	0.74	0.82

Text-Fig. 11. ▲△▲
U-stage microscope patterns of Om1, Zo1, Hbl1 and Pl.
XZ cuts parallel to lineation and perpendicular to foliation.
A: DR1 Om1 (S35, N = 80) in eclogite.
B: DR1 Zo1 (S35, N = 90) in eclogite.
C: DR1 Hbl1 in Grt amphibolite-mylonite (S32, N = 78).
D–F: DR2 Pl in layered amphibolite (S8, N_{D-F} = 113), G–I: DR2 Pl in granitic orthogneiss (SG1, N_{G-I} = 151) indicating (010) [001] glide operative in Pl.

Table 3. ◄◁◄
Microprobe analyses of Grt from Grt amphibolites (S26c, S32b). Locations: see Text-Fig. 2.

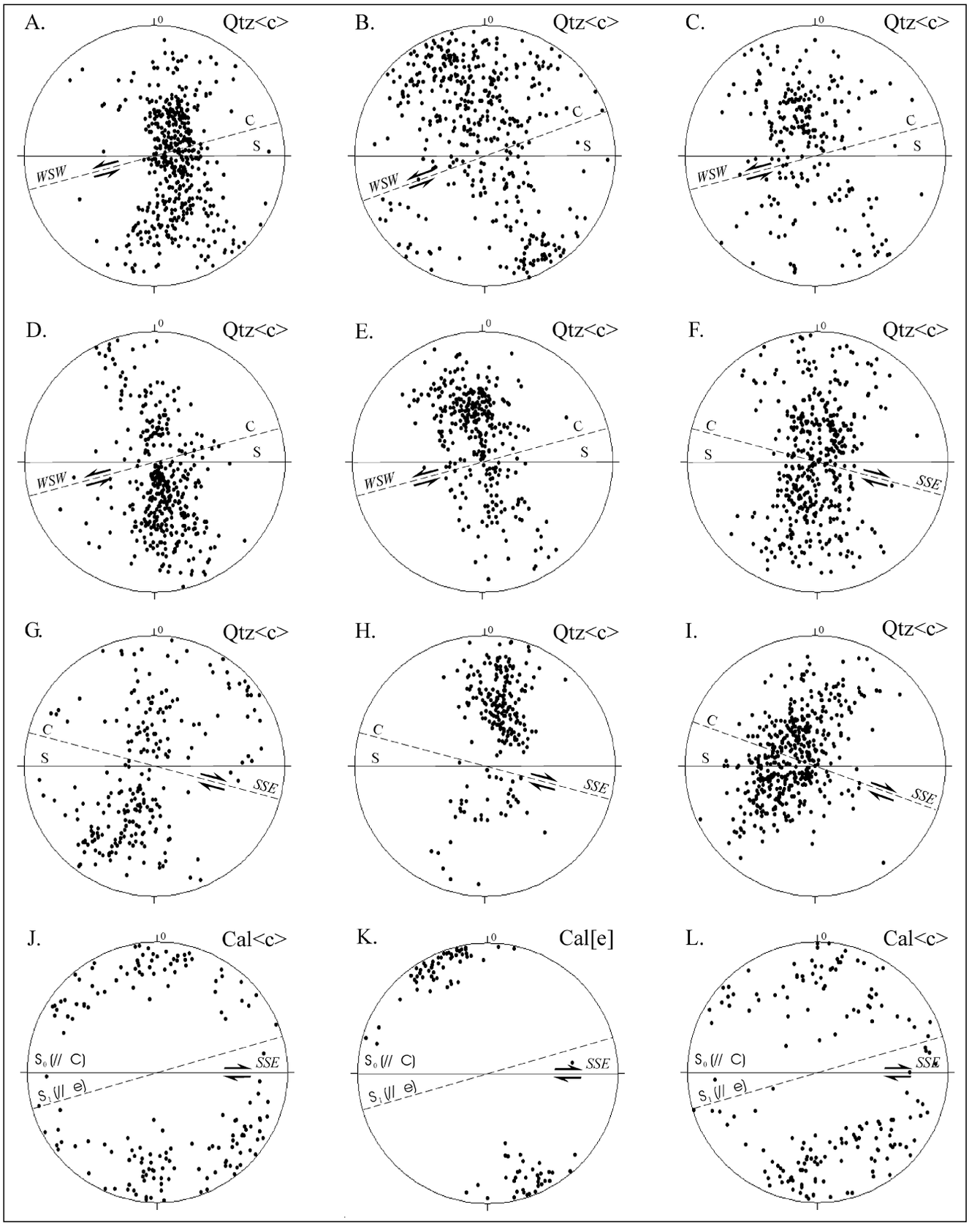

Text-Fig. 12.
U-stage microscope patterns of Qtz and Cal.
Qtz c-axes (A-I), Cal c-axes (J, L) and Cal e-poles (K) preferred orientation patterns. Grobgneis structural unit (A–E, DR3). Sieggraben structural unit (F-L, DR2), XZ cuts.

A,D,E: "Grobgneis" granitic mylonite (A-G3, N = 456; D-G13a, N = 403; E-G13b, N = 331).
B: Paragneiss mylonite (G4, N = 431).
C: Metaconglomerate mylonite (G5, N = 228).
F: Layered amphibolite (S8, N = 421).
G,I: Granitic orthogneiss mylonite (G-S12, N = 229, I-SG1, N = 461).
H: Metaquartzite mylonite in marble (S107, N = 229).
J–L: Marble (J-S11, N = 167; K-S11, N = 89; L-S11, N = 176).

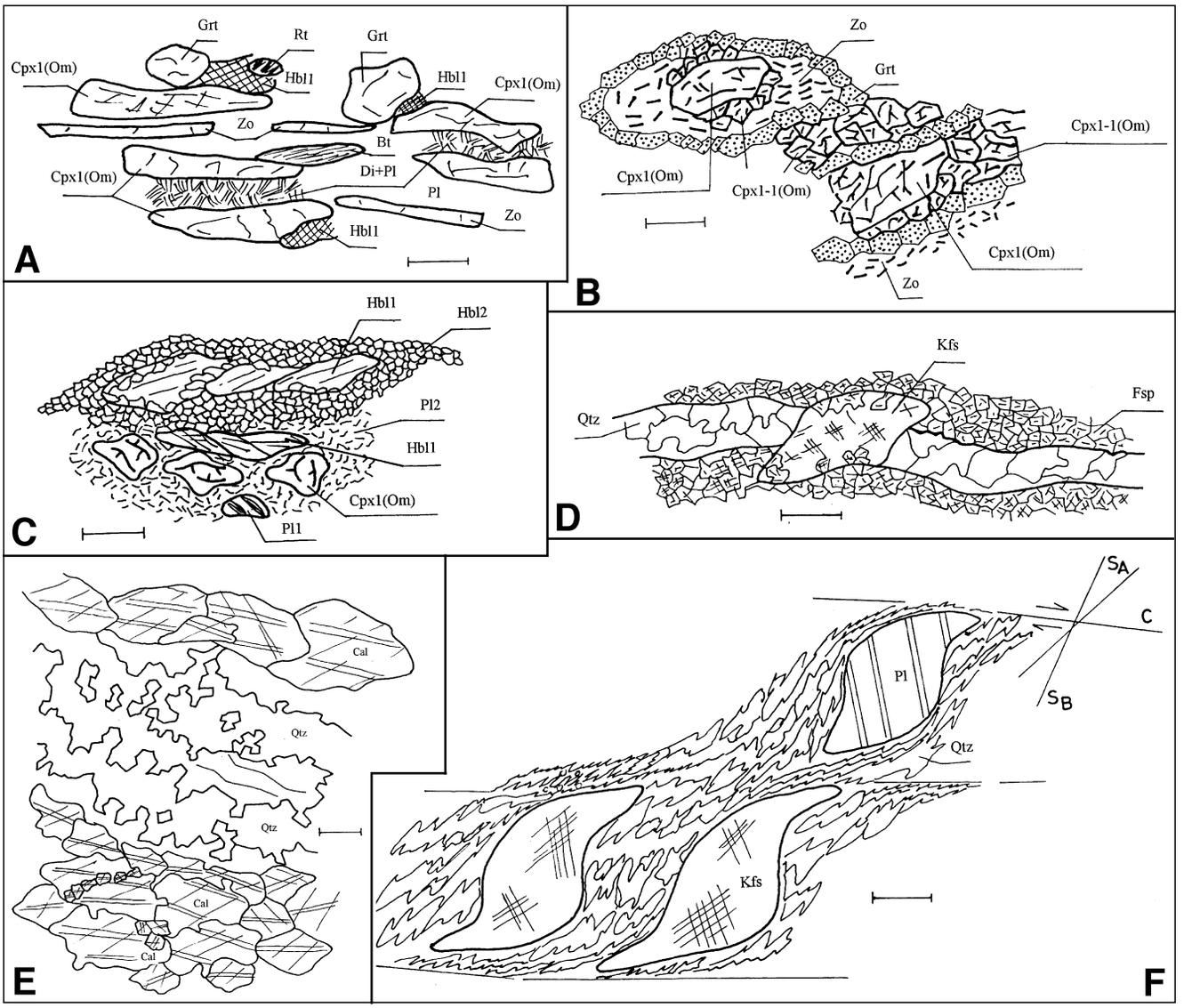

Text-Fig. 13.
Microtextures of mylonites of the Sieggraben and Grobgneis structural units from the different crustal levels.
A,B: Lower-crustal level: (DR1) eclogites (A), scale bar = 0.3 mm, and eclogitic mylonites (B), scale bar = 0.5 mm.
C,D: Mid-crustal level: (DR2) mylonites of amphibolized eclogites (C), scale bar = 0.3 mm, and granite-gneisses (D), scale bar = 0.5 mm.
E: Mid-upper crustal level: (DR2) mylonites of marbles with Qtz lenses and bands, scale bar = 1 mm.
F: Upper crustal level: (DR3) mylonites of Grobgneis-type granite-gneisses, scale bar = 1 mm.

ried out using the multicollector mass-spectrometer MAT-261. When model U-Pb ages were calculated, the Pb isotope composition was corrected for 0.20.1 ng "Pb blank" and for mass-discrimination 0.00130.0003 per mass unit. The model U-Pb ages and intercept of the discordia with concordia were calculated using LUDWIG's computer program (LUDWIG, 1991a,b). Calculation accuracy corresponds to 2σ.

3. Recrystallization P-T Path

The recrystallization P-T path (Text-Fig. 4) was reconstructed on the basis of changing rock-forming minerals, their composition and some thermo-barometric calculations applied in the different lithological members of the SSU.

The eclogite-bearing complex forms the middle part of the Sieggraben structural unit (SSU) (Text-Fig. 2). It comprises eclogites (Text-Fig. 8A–B) to amphibolites (Text-Fig. 8C–D) with thin bodies of serpentinites and rare flattened and boudinaged thin bodies of Opx-Ky-Grt-Hbl gneisses. Also boudinaged bodies (of centimeter to decameter, less than tens of meters) of eclogites are present in marbles and calc-silicate rocks (Text-Fig. 8E) due to the high viscosity contrast between the eclogites and enclosing country rocks. The whole lithological sequence is cut by veins a few metres thick of leucocrate granite to pegmatite altered to orthogneiss (Text-Fig. 8F). This is probably an Early Paleozoic basement complex with unknown Variscan metamorphic grade after a strong Alpine reactivation.

The progressive burial during subduction is reflected by the high-pressure prograde stage (DR1). On the climax of the prograde stage, depending on a bulk-rock chemistry, a part of the (meta)basites turned into mafic Cpx(Om)-Grt-Rt-Zo eclogites, and the other part into Pl-bearing eclogite-amphibolites or primary Grt amphibolites with pargasitic Hbl1. (Meta)pelites to psammites have turned into Grt-Ky gneisses and schists with high-pressure associations of Ky-Kfs-Ms-Qtz(Pl; (meta)limestones into impure marbles with low-Na Cpx(Di), Grt, Hbl, Ep and Scp; Mg-rich pelites into Opx-Ky-Hbl gneisses.

Table 4.
Microprobe analyses of minerals from the reaction domains of Grt amphibolites (S32b).
Cpx2 + Pl2 symplectites between the primary Hbl1 (Grt) and Qtz. *Fe_2O_3 and Fe^{3+} in Cpx2 calculated from site saturation and charge balance. Locations: see Text-Fig. 2.

Sample	S32b					
Phase	Grt			Hbl1	Cpx2	Pl2
	core	middle	rim			
SiO_2	38.85	38.95	39.13	44.54	52.90	60.48
TiO_2	0.05	0.14	0.10	0.69	0.12	-
Al_2O_3	21.66	21.54	21.74	12.63	0.62	24.58
FeO	22.57	22.63	23.40	15.61	9.96	-
MnO	0.67	0.87	0.67	0.23	0.16	-
MgO	4.77	4.73	5.23	10.75	12.88	-
CaO	11.32	11.09	9.68	10.66	23.13	6.35
Na_2O	-	-	-	2.48	0.19	8.09
K_2O	-	-	-	0.31	0.03	0.11
Fe_2O_3*	-	-	-	-	0.50	-
Total	99.92	99.95	99.95	97.90	100.49	99.61
Si	-	-	-	6.49	1.99	-
Al_{IV}	-	-	-	1.51	0.01	-
Al_{VI}	-	-	-	0.66	0.02	-
Ti	-	-	-	0.08	-	-
Fe^{3+}	-	-	-	0.61	0.01	-
Fe^{2+}	-	-	-	1.29	0.30	-
Mn	-	-	-	0.03	0.01	-
Mg	-	-	-	2.33	0.72	-
Ca	-	-	-	1.66	0.93	-
Na	-	-	-	0.70	0.01	-
K	-	-	-	0.06	-	-
Alm	48.8	49.0	51.1	Jd	-	
Sps	1.5	1.9	1.5	Ac	1.4	
Prp	18.4	18.3	20.3	Dp	69.9	
Grs	31.3	30.8	27.1	Hd	27,3	
				Ts	1.4	
X_{Fe}^{2+}	0.73	0.73	0.71	0.36	0.30	
					An	30.0

A prograde metamorphic trend from amphibolites to eclogites in the Eclogite-Amphibolite-Serpentinite-Marble Complex can be deduced after relic inclusions of Hbl1, Ep-Czo1 and Pl1 in Om (with 23–38 % of Jd, Tab. 1, Text-Fig. 5, 9A) or Grt grains; by a prograde zoning of some Grt grains in eclogites (Tab. 2), or at least in the central part of Grt in Grt amphibolites (Tab. 3, Text-Fig. 6). Grt amphibolites are depleted or devoided of Om, they contain primary Hbl1(Prg) (Tab. 4–6, Text-Fig. 7) coexisting with Grt (Tab. 4, Text-Fig. 9C) and Pl1. Some eclogites also contain relic Hbl1(Prg) (Tab. 6, Text-Fig. 7). Association of minerals like Om, Grt, Rt, Zo, Ab, Am formed during Early Alpine DR´1 HP/HT event (P = 14–15 kbar, at T ca. 700 °C) and indicates subduction of the probably Early Paleozoic basement (volcano-sedimentary) complex.

The mineral assemblage of marbles and calc-silicate rocks comprises low-Na Cpx, Am (brown-green), Scp, Ttn, but also Grt, Bt, Cal, Qtz and relics of Ep. Marbles contain layers of ophicalcite, marbles with serpentinized Fo, Grt(Adr-Grs), Cpx(Di) and Phl.

Some layers within metabasites have the character of high-grade Mg-rich gneisses (Qtz, Opx, Grt, Ky, Pl, DR2-1) with the retrograde Hbl 2(Ath) + Tcl in a metamorphic matrix (DR2-2).

The Gneiss Complex overlying the eclogite-bearing complex contains the higher amphibolite facies metamorphic mineral assemblage of the DR2-1 stage defined by Qtz, Bt (Tab. 7), Pl, Kfs, Ky, Grt (Tab. 7, Text-Fig. 6), Ms (rare inclusion in Grt).

The Micaschist Complex usually forms the top or the bottom of the Sieggraben unit. The micaschists contain Qtz, Bt, Ms, less Pl, Grt, Rt, Ilm, Tur and usually a high amount of opaque minerals. In the upper part of the complex there are micaschists interlayered by marbles (a few cm thick), usually as a part of dominant Cal-Ep-Bt(Am) gneisses.

A lot of veins and veinlets of Tur pegmatite caused tourmalinization and microclinization of micaschists.

On the retrograde stage eclogites were changed into amphibolized eclogites to amphibolites. The retrograde process can be subdivided into two P-T intervals DR2-1 and DR2-2. Decompression at slightly increased temperature in the initial stage of the uplift is reflected by reaction microtextures in form of Cpx 2 (with 20–5 % of Jd, Tab. 1, Text-Fig. 5, 9A) + Pl 2 (Olg to Ads, Tab. 4, 5) aggregates among Om (Tab. 1, Text-Fig. 5, 9A) grains in eclogites, or between pargasitic Hbl1 (Tab. 4–6, Text-Fig. 7, 9B) and Qtz in amphibolites. This is an Early Alpine DR2-1 HP/MP-HT stage of the uplift at T = 730–770°C and P $<$12 kbar.

High temperatures under decreasing pressures initiated segregation of pale layers of trondhjemite composition (Qtz, Pl, Am, Bt) in eclogite-amphibolites (Text-Fig. 8C), or of a granitic composition in high-grade gneisses (Qtz, Kfs, Pl, Ky, Bt, Sil).

Two types of high-T symplectite-bearing reactions characterize the earlier DR2-1 period of the uplift. Although the reactions were initiated by the uplift and pressure decrease, both represent a temperature increase related to extensional deformation. In the first type (Cpx 1 = Cpx 2 + Pl) at decreasing P and increasing T a newly-formed association Cpx 2 + Pl 2 (Text-Fig. 9A) has a larger volume than Cpx 1(Om) and the reaction was caused by decompression during the uplift (DR2). The second type (Hbl 1 + Qtz + Zo = Cpx 2 + Pl 2 + H_2O) represents a typical prograde dehydration reaction. The latter reaction is especially characteristic of Cpx 1-free Grt amphibolites (Text-Fig. 9B).

Table 5. Microprobe analyses of minerals from the reaction domains of Grt amphibolites (S26c). Cpx2 + Pl2 symplectites between the primary Hbl1 (Grt) and Qtz. *Fe_2O_3 and Fe^{3+} in Cpx2 calculated from site saturation and charge balance. Locations: see Text-Fig. 2.

Sample	S32b					S26c			
Phase	Hbl1	Cpx2	Pl2	Cpx2	Pl2	Hbl1		Cpx2	Pl2
SiO_2	44.43	54.68	66.97	53.40	65.93	45.63	41.88	53.67	63.24
TiO_2	0.59	0.15	-	0.26	-	0.96	0.63	0.13	-
Al_2O_3	13.44	3.23	14.06	5.58	23.85	12.43	17.32	1.58	23.22
FeO	14.97	7.30	-	7.42	-	11.80	13.80	4.83	-
MnO	0.16	0.11	-	0.14	-	0.13	0.14	-	-
MgO	10.40	12.15	-	11.20	-	13.42	10.66	14.74	-
CaO	11.24	20.50	3.83	20.63	4.32	10.90	10.88	22.66	3.93
Na_2O	2.20	2.00	6.06	1.89	5.47	2.53	2.70	0.87	9.45
K_2O	0.27	-	0.05	0.09	0.03	0.22	0.25	-	0.09
Fe_2O_3*	-	-	-	-	-	-	-	1.04	-
Total	97.70	100.12	100.97	100.61	99.60	98.03	98.26	99.47	99.84
Si	6.50	2.01	-	1.96	-	6.52	6.03	1.98	-
Al_{IV}	1.50	-	-	0.04	-	1.48	1.97	0.02	-
Al_{VI}	0.82	0.14	-	0.20	-	0.61	0.97	0.05	-
Ti	0.06	-	-	0.01		0.10	0.07	-	-
Fe^{3+}	0.35	-	-	-	-	0.58	0.71	0.03	-
Fe^{2+}	1.48	0.22	-	0.23	-	0.83	0.95	0.15	-
Mn	0.02	-	-	-	-	0.02	0.02	-	-
Mg	2.27	0.67	-	0.612	-	2.86	2.29	0.81	-
Ca	1.76	0.81	-	0.81	-	1.67	1.68	0.89	-
Na	0.62	0.14	-	0.13	-	0.70	0.75	0.06	-
K	0.05	-	-	-	-	0.04	0.05	-	-
Jd	-	15.2	-	16.2	-	-	-	3.3	-
Acm	-	-	-	-	-	-	-	2.9	-
Di	-	64.7	-	59.3	-	-	-	79.2	-
Hd	-	20.1	-	20.3	-	-	-	12.8	-
Ts	-	-	-	4.2	-	-	-	1.8	-
X_{Fe}^{2+}	0.39	0.25	-	0.27	-	0.22	0.29	0.16	-
An	-	-	25.8	-	30.4	-	-	-	18.6

Table 6. Microprobe analyses of Hbl1 (large grains associated with Cpx1, Grt, Ep, Pl1) from eclogite (S35b), eclogite-amphibolite (SW4/14, SW4/16) and Grt amphibolites without Cpx (S26c/1 – inclusion of Hbl1 in Grt core). Hbl2 analyses from rims around Grt in eclogite (SW4/16) and Grt amphibolite (S26c/2). Fe^{3+} calculated from site saturation and charge balance. Locations: see Text-Fig. 2.

Sample	S26c/1	S35b		SW4/14		SW4/16	S26c/2	SW4/16
Phase	Hbl1						Hbl2	
SiO_2	44.91	41.01	43.69	41.70	44.66	42.57	39.35	37.49
TiO_2	0.50	0.65	1.01	1.89	0.95	1.15	0.24	0.07
Al_2O_3	14.60	17.20	15.12	14.44	12.22	13.35	19.77	20.28
FeO	13.23	16.55	13.94	14.87	15.08	16.28	16.31	19.42
MnO	0.14	0.14	0.04	0.07	0.06	-	0.18	0.50
MgO	11.26	9.99	11.38	10.50	11.16	10.43	8.14	6.21
CaO	11.17	9.92	10.01	10.66	9.61	9.79	11.23	10.36
Na_2O	1.96	3.22	3.08	3.25	3.76	3.63	2.67	3.86
K_2O	0.12	0.66	0.64	0.54	0.64	0.89	0.24	0.22
Total	97.89	98.34	98.91	97.92	98.14	97.85	98.13	98.41
Si	6.46	5.94	6.25	6.14	6.52	6.27	5.77	5.58
Al_{IV}	1.54	2.06	1.75	1.86	1.48	1.73	2.23	2.42
Al_{VI}	0.93	0.88	0.80	0.65	0.62	0.59	1.18	1.14
Ti	0.05	0.07	0.11	0.21	0.10	0.13	0.03	0.01
Fe^{3+}	0.50	0.94	0.70	0.40	0.46	0.65	0.67	0.81
Fe^{2+}	1.09	0.94	0.97	1.43	1.38	1.35	1.32	1.61
Mn	0.02	0.02	-	0.01	0.01	-	0.02	0.06
Mg	2.41	2.16	2.42	2.30	2.43	2.29	1.78	1.38
Ca	1.72	1.54	1.53	1.68	1.50	1.54	1.76	1.65
Na	0.55	0.90	0.85	0.93	1.06	1.04	0.76	1.11
K	0.02	0.12	0.12	0.10	0.12	0.12	0.04	0.04
X_{Fe}^{2+}	0.31	0.30	0.29	0.38	0.36	0.37	0.43	0.54
X_{Fe}^{tot}	0.40	0.47	0.41	0.44	0.43	0.47	0.53	0.64

Further decompression and temperature-decrease (DR2-2-MP/LP-MT stage: T = 650–550°C, P <8 kbar) is indicated by blue-green tschermakite-rich Hbl between Grt and Om in eclogites (Tab. 6, Text-Fig. 7, 9A), or between Grt and pargasitic Hbl 1 in amphibolites (Tab. 6, Text-Fig. 7, 9C); Ilm and Ttn rims around Rt; Ath-Tlc rim around Opx in Opx-Hbl-Grt-Ky gneisses (Text-Fig. 9D); Pl-Hbl rim between Di and Ep, or Czo rim around Scp in marbles, amphibolization of Cpx in marbles and calc-silicate rocks; Bt 2 + Ky 2 or later Bt 2 + Sil 2 aggregates replacing Grt in dark bands at the presence of Kfs, and by recrystallized Ky 2 + Fsp 2 aggregates in the light-coloured bands of layered paragneisses.

During the medium-T stage of the uplift (DR2-2) were derived two retrograde reactions. Both reactions (Grt + Cpx1 + H_2O = Hbl ± Pl) in eclogites, or (Grt + Hbl ± Pl 1 + H_2O = Hbl 2) in Grt amphibolites represent the formation of a blue-green Al-enriched Hbl 2 ± Pl in contacts between Grt, Cpx 1 and Hbl 1 (Text-Fig. 9A–C).

Retrograde reactions in gneisses (Grt + Kfs + H_2O = Bt + Ky, then Grt + Kf + H_2O = Bt + Sil) belong to the typical isochemical hydration process.

The LT-period of the DR2 event is reflected by Qtz, Ser-Ms, Chl in gneisses and micaschists, or by Qtz, Chl, Act, Ep, Bt in amphibolites, although in general, it has a negligible extent within the internal part of the SSU. Low-temperature aggregates are especially bound to the C-(shear-)planes in S-C fabrics (BERTHÉ et al., 1979) developed near the basis of the SSU during the DR3 stage. Secondary Ms and Tur appeared in gneisses.

The complexes of the SSU survived a partly separate evolution since the DR1 (burial) event. The complex of metabasites, metaultrabasites and marbles indicates the deepest conditions of subductional burial (DR1 HP-HT event).

The suggested P-T (DR) path (Text-Fig. 4) is clearly common for eclogite-amphibolite-serpentinite-marble and gneiss complexes only since the peak temperature conditions that roughly fit for both complexes. They could be interpreted as starting conditions for an (early DR2) obduction-like exhumation of eclogite and gneiss bearing complexes. In that case, the complexes definitively must have been juxtaposed during the early DR2 collision-obduction event. The micaschist complex was exhumed separately from a shallower level.

Ten kilobars of decompression occurred during a temperature-decrease of approximately 200 °C. Such a minor temperature-decrease compared to decompression (Text-Fig. 4) suggests a rapid uplift and/or additional heat source during early Alpine (DR2) exhumation of the buried eclogite- and gneiss-bearing complexes (Text-Fig. 3). Both demands were met during an extensional mode of the exhumation (DR2).

Quite a rapid uplift of the Sieggraben structural unit can also be suggested by the practically missing low-T mineral assemblages. This feature is characteristic for all lithotectonic complexes of the SSU.

4. Relationship of Textural (CPO) Patterns to Macro- and Microstructures

Tectonostratigraphy of the MAA and LAA structural complexes as well as the field relationship of the superimposed macrostructures in the area considered are outlined in Text-Fig. 2.

The top of the tectonostratigraphic profile is occupied by the MAA Sieggraben structural unit (SSU) overlying the LAA Grobgneis and Wechsel ones, as the result of mid-Cretaceous collision (early-DR3 event). Internal structure of the Grobgneis unit comprises Permo-Scythian Bt-Chl metasandstones and metaconglomerates as well as Triassic metacarbonates of the cover as an evidence of Alpine juxtaposition of the previously described structural complexes (Text-Fig. 2).

The Late-DR3 (Late Cretaceous-Early Tertiary) extensional event also left distinct meso- and macrostructures in the whole tectonostratigraphic profile. The main tectonometamorphic overprint is recognizable in the hanging walls of the structural units. The S-C type of low-temperature mylonitic deformation is common there. The asymmetry of S and C planes indicates the top-to-WSW shearing along the distinct low-temperature mineral and stretching lineations. Lineation on C-planes is defined by the low-T newly formed minerals: WhM, Bt, Chl. Mesoscopic tension ("en-echelon" type) cracks are striking NW–SE. Low-angle normal faults in the hanging wall of the Grobgneis and Sieggraben structural units are representative macrostructures of the late-DR3 extensional event (Text-Fig. 2).

The older higher-temperature extensional (DR2, Early Cretaceous) fabrics are only recognizable in the internal part of the MAA Sieggraben structural unit. The unified NNW–SSE striking mineral and stretching lineations are characteristic for all lithological complexes of the SSU. Lineation is determined by the medium-T minerals like Am, e.g. in amphibolized eclogites. Newly-formed micas and ductilely deformed Fsp and Qtz aggregates define the lineation in granite-gneisses. Foliation is visible according to banded structures of eclogite-amphibolites, marbles, para- and ortho-gneisses (Text-Fig. 8B–F) indicating medium-T conditions of ductile deformation and recrystallization.

Microstructures of deforming minerals like omphacite, zoisite, amphibole, plagioclase, quartz and calcite (Text-Fig. 9, 10) are closely related to the P-T path (Text-Fig. 4) of the (DR2) extensional uplift.

The dynamic recrystallization of originally prismatic Om 1 (Text-Fig. 13A) into an aggregate of Om 2 in layered structures of eclogites (Text-Fig. 8B) was accompanied by synkinematic growth of Grt2 in ranges enclosing core-mantle structures of flattened Om1 porphyroclasts in mylonitic foliation (Text-Fig. 13B). Similarly, Zo1 is altered into dynamically recrystallized bands of Zo2 (Text-Fig. 13B). Such HT/HP microstructures might reflect an initial uplift (early DR2) of eclogites from the lower crustal level just after the subduction (DR1).

The Early Alpine period of extension (DR2 event) mainly left the medium-temperature mylonites of all rock types of the MAA Sieggraben structural unit, which are characteristic of the mid-crustal level:

Strongly amphibolized eclogites (gabbro-eclogites, Text-Fig. 8A–B) to layered amphibolites (Text-Fig. 8C–D) show a distinct NNW–SSE mineral and stretching lineations defined by partially re-oriented shaped preferred Om 1 (N_Z optical directions, Text-Fig. 11A), Zo 1 (N_X, Text-Fig. 11B) and Am 1 (c-axes, Text-Fig. 11C; Text-Fig. 13A) crystals. E.g. Cpx-Om 1 appears to be a "hard" mineral phase enclosed in mylonitic matrix (Text-Fig. 13B). Passive Cpx markers within a ductile matrix of Hbl and Pl are segmented by a lot of tension fractures and microshears (Text-Fig. 13C). Hbl and Pl with low viscosity contrast underwent distinct dy-

Table 7. Microprobe analyses of zonal Grt with Bt inclusions from Bt-Grt gneiss (S16b). Location: in Text-Fig. 2.

Sample	S16b							
Phase	Grt	Bt	Grt	Bt	Grt	Bt	Grt	Bt
	core		middle		middle		rim	
SiO_2	38.35	37.15	37.66	37.38	38.04	37.40	38.04	38.38
TiO_2	0.13	4.56	-	3.77	0.04	4.74	-	4.59
Al_2O_3	21.26	16.65	21.32	15.76	21.37	17.25	21.73	17.83
FeO	28.14	16.70	29.61	17.54	30.16	15.64	30.91	13.13
MnO	1.18	-	1.41	-	1.43	-	1.54	-
MgO	4.36	11.97	4.00	12.75	4.29	12.11	5.06	13.07
CaO	5.34	-	5.90	0.09	4.53	-	2.62	0.02
Na_2O	-	-	-	0.09	-	-	-	0.21
K_2O	-	9.11	-	9.32	-	9.39	-	9.43
Total	99.76	96.14	99.90	96.70	99.86	96.53	99.90	96.46
Alm	64.8	-	64.7	-	66.9	-	68.9	-
Sps	2.7	-	3.1	-	3.2	-	3.5	-
Prp	17.3	-	15.6	-	17.0	-	20.1	-
Grs	15.2	-	16.6	-	12.9	-	7.5	-
Si	-	2.83	-	2.83	-	2.83	-	2.88
Al_{IV}	-	1.17	-	1.17	-	1.17	-	1.12
Al_{VI}	-	0.33	-	0.24	-	0.37	-	0.44
Ti	-	0.26	-	0.21	-	0.27	-	0.26
Fe	-	1.06	-	1.11	-	0.99	-	0.83
Mg	-	1.35	-	1.44	-	1.37	-	1.47
Na		-	-	0.02	-	-	-	0.03
K	-	0.89	-	0.87	-	0.91	-	0.91
X_{Fe}	0.79	0.44	0.81	0.44	0.80	0.42	0.77	0.36

namic recrystallization in amphibolites. Hbl porphyroclasts are surrounded with mantle structures and long tails of dynamically recrystallized aggregates (Text-Fig. 13C). Deformation (100) twins, kink bands, tension gashes, microfaults and book-shelf structures of Hbl are common. Pl is intensively dynamically recrystallized into fine grained ultramylonitic layers (Text-Fig. 13C). Microstructures of Hbl and Pl suggest dislocation creep as active deformation mechanism. Grain boundary sliding or superplastic flow could operate in extremely fine-grained ultramylonitic bands of Pl.

Plagioclase (mostly with 9–16 An content) N_X (Text-Fig. 11D), N_Y (Text-Fig. 11E) and N_Z (Text-Fig. 11F) optical directions that were measured from the light-coloured bands of amphibolites indicate a slip activity in the {010}[001] system close to foliation and lineation. An almost pure-shear regime of deformation can be supposed, because of an acute angle of optical (N_Y) and planar {010} crystallographic elements to foliation and lineation. A prism <a> glide system (LIASTER & HOBBS, 1980; SCHMID & CASEY, 1986) predominated in Qtz (Text-Fig. 12F).

Mylonitic granite-gneisses (Text-Fig. 8F, 10A, 13D) show dynamic recrystallization of Fsp and migration recrystallization of Qtz to ribbons. Some Fsp porphyroclasts are rimmed by the newly-formed subgrains. Asymmetric "mica-fish" structures of Ms (Text-Fig. 10A) indicate a general top-to-the SSE extensional sliding during the exhumation (DR2). Large flakes of Ms are partially replaced by fine-grained recrystallized aggregate of the WhM. Pl (with 5–16 An content) N_X (Text-Fig. 11G), N_Y (Text-Fig. 11H), N_Z (Text-Fig. 11I) and Qtz c-axes (Text-Fig. 12G, I) preferred orientation patterns resemble those patterns from layered amphibolites (Text-Fig. 11E–F, 12F). Dislocation creep in the {010}[001] glide system occurred in Pl; prism <a> with the contribution of the rhomb glide systems was active in Qtz.

Calcite in marbles (Text-Fig. 8E, 10C) exhibits an internal medium- to low-temperature e-lamellae parallel to flattened grains and oblique to C-planes with dynamically recrystallized Cal(2) grains within the shear bands (the top and bottom of Text-Fig. 10C). Calcite e-poles (Text-Fig. 12K), c-axes (Text-Fig. 12J,L) indicate the po-

Table 8.
U-Pb isotopic data for uranium containing minerals from metagranites of the Sieggraben structural unit (to Fig. 14A).
[1]) Measured ratios.
[2]) Data corrected for mass-discrimination, blank and common lead.
[3]) The isotope composition of common lead for correction of $^{207}Pb/^{206}Pb$ was determined in feldspars (Fsp) after their washing by HNO_3. For Fsp SG-1 it corresponds to $^{206}Pb/^{204}Pb = 19.111$, $^{207}Pb/^{204}Pb = 38.534$ and for Fsp SW-2 it corresponds to $^{206}Pb/^{204}Pb = 18.507$, $^{207}Pb/^{204}Pb = 15.672$, and for $^{208}Pb/^{204}Pb = 38.493$.

Mineral-Sample	U (ppm)	Pb (ppm)	$\frac{^{206}Pb}{^{204}Pb}$ [1]	$\frac{^{206}Pb}{^{207}Pb}$ [1]	$\frac{^{206}Pb}{^{208}Pb}$ [1]	$\frac{^{206}Pb}{^{238}U}$ [2] (%)	$\frac{^{207}Pb}{^{235}U}$ [2] (%)	Rho	$\frac{^{207}Pb}{^{206}Pb}$ [3] (Ma)
Zr-SG-1	3513	103.6	780.3	14.326	17.1812	0.02972±0.31	0.20956±0.43	0.75	247.4±6.5
Ap-SG-1	41.2	7.96	25.85	1.6211	0.65784	0.01820±0.89	0.1254±13.8	0.93	-
Zr-SW-2	3058	136	285.4	9.6924	6.88892	0.03870±0.31	0.27796±0.39	0.82	289.7±5.1
Mnz-SW-2	10590	1216	3533	17.811	0.44994	0.04024±0.32	0.28896±0.35	0.92	289.1±3.2
Mnz-SW-2a	3584	388.7	281.2	9.6243	0.54973	0.04005±0.36	0.28747±2.98	0.59	287.8±64

sition of the compression tensor $\sigma 1$ that acted almost subvertically during the Early Alpine (DR2) exhumation period connected with the top-to-the SSE extension shearing of the MAA basement.

Microstructures of Qtz lenses and bands in marble (Text-Fig. 12H, 13E) indicate a dislocation creep in the prism <a> glide system and migration recrystallization to ribbons (1) during the medium-T period of the DR2 extensional deformation. The next period is represented by oblique small ribbons (2) within the ribbons (1). The lower temperature and higher deformation rate caused dynamic polygonization of the ribbon (1)/(2) boundaries that are at last cut by very low-T tension fractures filled by Cal. Thus the deformation of Qtz was controlled by plastic deformation of host (Cal) marble.

P-T and deformation paths indicate a rapid uplift of the SSU probably by an obduction-like process (DR2) (Text-Fig. 3) in form of a collision-driven extension exhumation. The result of ongoing mid-Cretaceous collision (early-DR3 event) was the thrust of the MAA Sieggraben unit over the LAA structural units (Text-Fig. 2, 3). The microstructures of this compressional deformation were strongly modified by a newer Late Cretaceous–Early Tertiary extension (late-DR3 event) that started the unroofing of the Pennine and LAA units (Text-Fig. 3). Especially the submerged LAA units suffered LT mylonitization. E.g. the mylonitic granite-gneiss or "Grobgneis" reveals a top-to-the WSW extension shearing with a perfect ductility of Qtz and a semi-ductility of Fsp (Text-Fig. 10B, 13F).

Asymmetric Qtz c-axes patterns (Text-Fig. 12A–E) are the result of combined basal <a> and prism <a> glides. The distinct S-C fabrics (BERTHÉ et al., 1979) confirm a top-to-the WSW shearing during the late-DR3 event. The local pseudotachylitic textures (Text-Fig. 10D), e.g. in Grobgneis-type granite gneiss suggest their development in a seismoactive level. Some asymmetric quartz c-axes patterns in the hanging wall of the Sieggraben structural unit are consistent with the superimposed DR3 top-to-the WSW extensional shearing.

5. Discussion and Conclusions

The analysis of deformation-recrystallization stages (DR1-3) of the Middle Austro-Alpine (MAA) eclogite-bearing Sieggraben structural unit (= SSU) revealed a polyphase evolution of the AA internides (Text-Fig. 1–3).

The Early Alpine A-type subduction (DR1, HP/HT event: P = 14–15 kbar, at T ca. 700°C) predated a collision-driven exhumation (DR2) constrained by the dominating Early Cretaceous isotope ages of 137±1–109.3±1 Ma (^{40}Ar–^{39}Ar plateau data on amphiboles from amphibolites [DALLMEYER et al., 1992, 1996]), or 103±14 Ma (U-Pb-lower discordia intercept using zircon and monazite from granite-gneisses [PUTIŠ et al., 1994, and this paper]). This time period overlaps with the period of shortening within the Meliata-Hallstatt passive continental margin.

The reconstructed P-T path (Text-Fig. 4), as well as the changes in mineral composition (Text-Fig. 5–7) and the reaction microstructures (DR2, Text-Fig. 9) of eclogites, amphibolites, marbles and gneisses reflect decompression at a slightly arised temperature (almost an isothermal decompression) at least during the first period of the uplift: DR2-1-HP/MP-HT stage: T = 730–770 °C, P $<$12 kbar, or a simultaneous decrease of temperature with pressure during the DR2-2-MP/LP-MT stage: T = 650–550 °C, P $<$8 kbar. Ten kilobars of decompression occurred during a temperature-decrease of approximately 200°C. Such a minor temperature-decrease compared to the decompression (Text-Fig. 4) was enabled by the extensional conditions of the uplift during the Early Alpine (DR2) exhumation (Text-Fig. 3). The rate of the uplift was controlled both by the rate of mineral reactions, and the rate of ductile (dislocation recovery, or power-law) deformation (BARBER, 1990). There is a characteristic change of rheologically active minerals along the P-T-t loop during a few deformation-recrystallization stages of the uplift through the different lithospheric levels. The latter argument, however, does not point to an extremely high rate of exhumation. There was enough time for both the mineral reactions and the dynamic recrystallization of rheologically active phases in the ductile shear zone.

The complexes of the SSU survived a partly separated evolution. The only complex of metabasites, metaultrabasites and marbles clearly preserves HP-HT mineral associations after subduction (DR1). The relics of higher-pressure mineral association (Ky-Kfs-Qtz) in high-grade gneisses could indicate their burial into the subduction zone too. The complexes were definitively juxtaposed into one structural unit (SSU) during (early DR2) obduction-collision event. The estimated P-T-DR path (Text-Fig. 4) is common for eclogite-amphibolite-serpentinite-marble- and gneiss complexes only since the DR2 stage. The micaschists were exhumed from a shallower level as an independent complex.

A footwall propagating a master detachment fault, combined with the hanging wall structural unroofing was responsible for the exhumation of the SSU. The exhumation process was firstly accommodated by dynamic strain softening in pyroxene (Om) and zoisite aggregates in eclogites at the lower-crustal level. Dynamic recrystallization of feldspars, amphibole and migration quartz ribbon fabrics of granite-gneisses and layered amphibolites indicate a superimposed mid-crustal rheology during a top-to-the SSE extensional shearing (DR2) and uplift of the SSU. Consequently of this part of the eclogites is wrapped by ductile host rocks, mainly by banded amphibolites, protecting them against a stronger deformation and retrograde recrystallization.

Textural patterns suggest a pronounced preferred orientation of Om1 and Zo1 in lineation and foliation as the result of oriented metamorphic (DR1) growth in eclogites. Other minerals like Om2, Zo2, Pl, Kfs, Qtz and Cal bear the features of ductile deformation of amphibolites, granite-gneisses and marbles by micromechanisms of dislocation flow in both coaxial and noncoaxial tectonic regimes. Their textural patterns reveal predominant medium-T prism <a>, less rhomb glide (early DR2), or a low T basal <a> glide (late DR2 and DR3) in Qtz. The {010}[001] system was active in Pl (DR2). Cal low-T (late DR2) e-lamellae indicate the mechanical twinning as the main deformation micromechanism, with the negligible contribution of dislocation flow and dynamic recrystallization in the C-planes. Asymmetry of crystallographic preferred orientation (CPO) patterns is consistent with the asymmetry of mesostructures (e.g. S-C mylonites) and both confirm the DR2 top-to-the SSE, or DR3 top-to-the WSW shearing (Text-Fig. 12, 13).

U-Pb analytical data of dated Sieggraben orthogneiss are outlined in Tab. 8. A concordia diagram for Zr and Mnz is depicted in Text-Fig. 14A. The upper concordia intercept with discordia (312.7±7.9 Ma) is interpreted as the age of magmatic emplacement of the granite veins

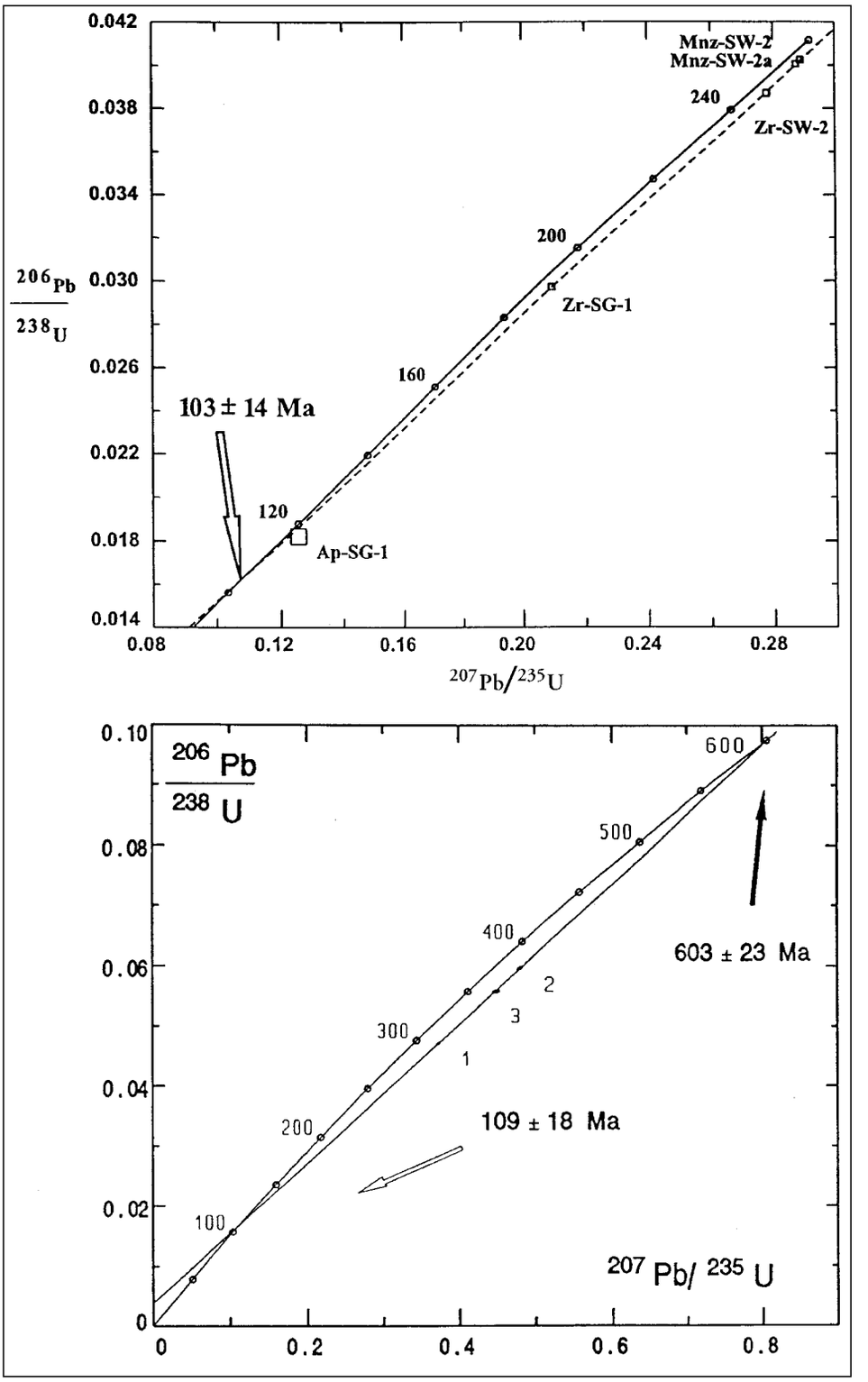

Text-Fig. 14.
Concordia diagrams for some uranium-containing minerals.
A: Sample SW2 (3 points: one Zr and two Mnz) and sample SG1 (2 points: Zr and Ap). Both samples are granitic orthogneisses of the MAA Sieggraben structural unit.
B: Sample W1 (3 points of Zr), the LAA Wiesmath orthogneiss.

into an Early Paleozoic (Variscan) complex. This is compatible with the WR Rb-Sr age of 289±16 Ma from the same sample (PUSHKAREV in PUTIŠ et al., 1994). The lower intercept (103±14 Ma) age is interpreted to date a higher-temperature metamorphic event, with the real temperatures above the blocking ones of U-Pb isotope system in Zr and Mnz. Such conditions correspond to those achieved during the DR2 stage (770–550°C), as it is proved by petrological data. Although the granite-pegmatite veins discordantly cut the metabasite-marble complex, both have a common (Alpine) metamorphic-mylonitic fabric. From this point of view, the lower intercept age can be related to deep-crustal thrusting of the SSU over the LAA structural complexes during the DR2 stage.

A similar intercept age of 109±18 Ma (Text-Fig. 14B, after KOTOV in KORIKOVSKY et al., 1998) was obtained from Zr of the Lower AA Wiesmath orthogneiss (a locality near Wiesmath) of the Wechsel structural unit. This age is interpreted to date the Alpine metamorphism climax conditions (T 500°C at P 10 kbar [KORIKOVSKY et al., 1998]) in the buried footwall LAA structural complex.

The Late Cretaceous-Early Tertiary collision-related extensional event (DR3, K-Ar data: Ms 88±5–76±4 Ma, Kfs 97±5–88±4 Ma, Bt 78±6 Ma [PUSHKAREV in PUTIŠ et al., 1994]) thus followed the closure of the Penninic Ocean. It enhanced the exhumation of buried LAA (and Pennine) structural complexes in some domes and tectonic windows. This event, or a top-to-the WSW extensional shearing was mainly controlled by the low-T quartz rheology. Although it is penetrative for the LAA structural complex, only the basis of the SSU was reactivated.

Acknowledgements

The authors wish to express their gratitude for the fundation of the field and laboratory works to the directorate of the Geological Survey of Austria in Vienna. The manuscript was improved thanks to critical and helpful comments of colleagues H. STÜNITZ, F. NEUBAUER, and two unknown reviewers.

References

BARBER, D.J., 1990: Regimes of plastic deformation – processes and microstructures: an overview. – In: BARBER, D.J. & MEREDITH, P.G. (Eds.): Deformation processes in minerals, ceramics and rocks, 423 p., 138–177, London (Unwin Hyman).

BERTHÉ, D., CHOUKROUNE, P. & JEQUOZO, P., 1979: Orthogneiss, mylonite and non-coaxial deformation in granites: The example of the South Armorican shear zone. – J. Struct. Geol., **1**, 31–42.

BLUNDY, J.D. & HOLLAND, T.J.B., 1990: Calcic amphibole equilibria and a new amphibole-plagioclase geothermometer. – Contrib. Mineral. Petrol., **104/2**, 208–224.

DALLMEYER, R.D., NEUBAUER, F., HANDLER, R., MÜLLER, W., FRITZ, H., ANTONITSCH, W. & HERMANN, S., 1992: 40Ar/39Ar and Rb-Sr mineral age controls for the Pre-Alpine and Alpine tectonic evolution of the Austro-Alpine nappe complex, Eastern Alps. – In: NEUBAUER, F. (Ed.): ALCAPA-Field Guide, Univ. Graz, 47–59.

DALLMEYER, R.D., NEUBAUER, F., HANDLER, R., FRITZ, H., MÜLLER, W., PANA, D. & PUTIŠ, M., 1996: Tectonothermal evolution of the internal Alps and Carpathians: Evidence from 40Ar/39Ar mineral and whole-rock data. – Eclogae geol. Helv., **89/1**, 203–227.

ECKERT, J.D., Jr., NEWTON, R.C. & KLEPPA, O.J., 1991: The delta H of reaction and recalibration of garnet-pyroxene-plagioclase-quartz geobarometers in the CMAS system by solution calorimetry. – Amer. Min., **76**, 1/2, 148–160.

FRANK, W., KRALIK, M., SCHARBERT, S. & THÖNI, M., 1987: Geochronological data from the Eastern Alps. – In: FLÜGEL, H.W. & FAUPL, P. (Eds.): Geodynamics of the Eastern Alps, 272–281 (Deuticke) Vienna.

FRISCH, W. & NEUBAUER, F., 1989: Pre-Alpine terranes and tectonic zoning in the Eastern Alps. – Geol. Soc. Am. Sp. Pap., **230**, 91–100.

GRAHAM, C.M. & POWELL, R.H., 1984: A garnet-hornblende geothermometer; calibration, testing and application to the Pelona Schists, Southern California. – J. Metam. Geol., **2/1**, 33–42.

HOLLAND, T.J.B., 1980: The reaction albite = jadeite + quartz determined experimentally in the range 600–1200°C. – Amer. Min., **65**, 129–134.

HOLLAND, T.J.B. & BLUNDY, J.D., 1994: Non-ideal interactions in calcic amphiboles and their bearing on amphibole-plagioclase thermometry. – Contrib. Mineral. Petrol., **116**, 433–447.

KOHN, M.Y. & SPEAR, F.S., 1989: Empirical calibration of geobarometers for the assemblage garnet + hornblende + plagioclase + quartz. Amer. – Min., **74**, 1/2, 77–84.

KOTOV, A., MIKO, O., PUTIŠ, M., KORIKOVSKY, S.P., SALNIKOVA, E.B., KOVACH, V.P., YAKOVLEVA, S., BEREZNAYA, N.G., KRÁL, J. & KRIST, E., 1996: U/Pb dating of zircons of postorogenic acid metavolcanics and metasubvolcanics: A record of Permian-Triassic taphrogeny of the West-Carpathian basement. – Geol. Carpath., **47/2**, 73–79.

KORIKOVSKY, S.P., PUTIŠ, M., KOTOV, A.B., SALNIKOVA, E.B. & KOVACH, V.P., 1998: High-pressure metamorphism of the phengite gneisses of the Lower Austroalpine nappe complex in the Eastern Alps: mineral equilibria, P-T parameters, age. – Petrology **6/4**, 603–619.

KOZUR, H., 1991: The geological evolution at the western end of the Cimmerian ocean in the Western Carpathians and Eastern Alps. – Zbl. Geol. Paläont., T. 1, H. **1**, 99–121.

KROGH, E.Y., 1988: The garnet-clinopyroxene Fe-Mg geothermometer: a reinterpretation of existing experimental data. – Contrib. Mineral. Petrol., **99/1**, 44–48.

KMEL, F., 1935: Die Sieggrabener Deckscholle im Rosaliengebirge (Niederösterreich-Burgenland). – Tscherm. Mineral. Petrol. Mitt., **47**, 141–184.

LISTER, G.S. & HOBBS, B.E., 1980: The simulation of fabric development during plastic deformation and its application to quartzite: the influence of deformation history. – J. Struc. Geol., **2**, 355–370.

LUDWIG, K.R., 1991a: PbDat for MS-DOS, version 1.21. – U.S. Geol. Survey Open-File Rept., 88–542, 1–35. LUDWIG, K.R., 1991b: ISOPLOT for MS-DOS, version 2.50. – U.S. Geol. Survey Open-File Rept., 88–557, 1–64.

MANBY, G.M. & THIEDIG, F., 1988: Petrology of eclogites from the Saualpe, Austria. – Schweiz. Mineral. Petrogr. Mitt., **68**, 441–446.

MANBY, G.M., THIEDIG, F. & MILLAR, I., 1989: Textural, chemical and isotopic constraints on the age of the Saualpe eclogites (Carinthia/Austria). – In: SASSI, F.P. & BOURROUILH, R. (Eds.): IGCP 5, Newslet. **7**, 195–202.

MATTE, Ph., 1986: Tectonics and plate tectonics model for the Variscan belt of Europe. – Tectonophysics, **126**, 329–374.

MATTE, Ph., 1991: Accretionary history and crustal evolution of the Variscan belt in Western Europe. – Tectonophysics, **196**, 309–337.

MCKENNA, L.W. & HODGES, K.V., 1988: Accuracy versus precision in locating reaction boundaries: implications for the garnet-plagioclase-aluminium silicate-quartz geobarometer. – Am. Miner., **73**, 9/10, 1205–1208.

NEUBAUER, F., 1994: Kontinentkollision in den Ostalpen. – Geowissenschaften, **12**, 5/6, 136–140.

NEUBAUER, F., MÜLLER, W., PEINDL, P., MOZSCHEWITZ, E., WALLBRECHER, E. & THÖNI, M., 1992: Evolution of lower Austroalpine units along the eastern margins of the Alps: a review. – In: NEUBAUER, F. (Ed.): ALCAPA Field Guide, Univ. Graz, 97–114.

NEUBAUER, F. & FRISCH, W., 1993: The Austroalpine metamorphic basement east of the Tauern window. – In: VON, RAUMER, J.F. & NEUBAUER, F. (Eds.): Pre-Mesozoic Geology in the Alps. Springer-Verlag, Berlin, 515–536.

NEUBAUER, F., FRITZ, H., BOJAR, A.-V., JANÁK, M., PUTIŠ, M. & REICHWALDER, P., 1993: Kinematics of a blueschist-bearing nappe: the Meliata unit of the Western Carpathians. – Terra abstracts, Abstr. suppl. No. 2 to Terra nova, **5**, 24.

NEUBAUER, F. & VON RAUMER, J.F., 1993: The Alpine basement – linkage between Variscides and East-Mediterranean Mountain Belts. – In: VON, RAUMER, J.F. & NEUBAUER, F. (Eds.): Pre-Mesozoic Geology in the Alps, 515–536 (Springer-Verlag) Berlin.

PATTISON, D.R.M. & NEWTON, R.C., 1989: Reversed experimental calibration of the garnet-clinopyroxene Fe-Mg exchange thermometer. – Contrib. Mineral. Petrol., **101**, 1, 87–103.

PERKINS, D.I. & NEWTON, R.C., 1981: Charnockite geobarometers based on coexisting garnet-pyroxene-plagioclase-quartz. – Nature, **292/9**, 144–146.

PLAŠIENKA, D., 1991: Mesozoic tectonic evolution of the epi-Variscan continental crust of the Central Western Carpathians – a tentative model. – Mineralia slovaca, **23**, 447–457.

PLAŠIENKA, D., 1993: Structural pattern and partitioning of deformation in the Veporic Foederata cover unit (Central Western Carpathians). – In: RAKÚS, M. & VOZÁR, J. (Eds.): Geodynamic model and deep structure of the Western Carpathians, Conf., Symp., Sem., D. Štúr Inst. Geol., Bratislava, 269–277.

PLAŠIENKA, D. & PUTIŠ, M., 1993: Kinematics of Cretaceous uplift of the Veporic dome (Western Carpathians). – Terra abstracts, Abstr. suppl. No. 2 to Terra nova, **5**, 27.

PLAŠIENKA, D., GRECULA, P., PUTIŠ, M., HOVORKA, D. & KOVÁC, M., 1997: Evolution and structure of the Western Carpathians: an overview. – In: GRECULA, P., HOVORKA, D. & PUTIŠ, M. (Eds.): Geological evolution of the Western Carpathians, Monograph, Mineralia Slovaca Press, Bratislava, 1–28.

POWELL, R.H., 1985: Retrogression diagnostics and robust regression in geothermometer/geobarometer calibration: the garnet-clinopyroxene geothermometer revised. – J. Met. Geol., **3**, 3, 231–243.

PUTIŠ, M., 1991: Tectonic styles and Late Variscan–Alpine evolution of the Tatric-Veporic crystalline basement in the Western Carpathians. – Zbl. Geol. Paläont., T. 1, H. **1**, 181–204.

PUTIŠ, M., 1992a: Bericht 1991 über geologische Aufnahmen im kristallinen Grundgebirge auf Blatt 107 Mattersburg. – Jb. Geol. B.-A., **135/3**, 725–726.

PUTIŠ, M., 1992b: Variscan and Alpidic nappe structures of the Western Carpathian crystalline basement. – Geol. Carpath., **43/6**, 369–380.

PUTIŠ, M., 1994: South Tatric-Veporic basement geology: Variscan nappe structures; Alpine thick-skinned and extensional tectonics in the Western Carpathians (Eastern Low Tatra Mts., Northwestern Slovak Ore Mts.). – Mitt. österr. Geol. Ges., **86**, 83–99.

PUTIŠ, M., 1995: Deformation-recrystallization process within the shear zones: Tatro-Veporic Zone of the Western Carpathians; Middle-Austroalpine Sieggraben Unit of the E. Alps. – Habil. thesis Comenius Univ., Bratislava (in Slovak).

PUTIŠ, M. & KORIKOVSKY, S.P., 1993: From subduction to Tertiary uplift history: metamorphism, thrust and extensional tectonics of the Sieggraben unit, E. Alps. – Terra abstracts, Abstr. suppl. No. 2 to Terra nova, **5**, 28.

PUTIŠ, M., KORIKOVSKY, S.P., PUSHKAREV, Y.A. & ZAKARIADZE, G.S., 1994: Geology, tectonics, petrology, geochemistry and isotope dating of the Sieggraben (Grobgneis and Wechsel) Unit in the Eastern Alps. – Manuscript, Geological Survey of Austria, Vienna.

PUTIŠ, M. & KORIKOVSKY, S.P., 1995: Rheological-petrological path of the eclogite-, marble-, gneiss-bearing complexes during extensional uplift (the Sieggraben unit, Middle Austroalpine, Eastern Alps). – In: SCHULMANN, K. & VRÁNA, S. (Eds.): Thermal and Mechanical Interactions in Deep Seated Rocks, J. Czech Geol. Soc., Abstract Vol., **40/3**, 38–39.

SCHMID, S.M. & CASEY, M. 1986: Complete fabric analysis of some commonly observed quartz c axis patterns. – In: HOBBS, B.E. & HEARD, H.C. (Eds.): Mineral and Rock Deformation: Laboratory Studies, Geoph. Monogr. Ser., **36**, 263–286.

SCHUMACHER, J.C., 1991: Empirical ferric iron corrections: necessity, assumptions, and effect on selected geothermobarometers. – Min. Mag., **55**, 3–18.

STAMPFLI, G.M., 1996: The Intra-Alpine terrain: A Paleotethyan remnant in the Alpine Variscides. – Eclogae Geol. Helv., **89**, 13–42.

THÖNI, M. & JAGOUTZ, E., 1992: Some new aspects of dating eclogites in orogenic belts: Sm-Nd, Rb-Sr, and Pb-Pb isotopic results from the Austroalpine Saualpe and Koralpe type-locality (Carinthia/Styria, southeastern Austria). – Geochim. Cosmochim. Acta, **56**, 347–368.

THÖNI, M. & JAGOUTZ, E., 1993: Isotopic constraints for eo-Alpine high-P metamorphism in the Austroalpine nappes of the Eastern Alps: bearing on Alpine orogenesis. – Schweiz. mineral. petrogr. Mitt., **73**, 177–189.

TOLLMANN, A., 1977: Geologie von Österreich. Band I: Die Zentralalpen . – 766 pp., (Deuticke) Vienna.

Mineral Abbreviations in Text and Text-Figures

Ab	albite	Ktp	kataphorite
Acm	acmite	Kfs	kalifeldspar
Act	actinolite	Ky	kyanite
Adr	andradite	Mnz	monazite
Ads	andesine	Ms	muscovite
Aeg	aegirine	Olg	oligoclase
Alm	almandine	Om	omphacite
Am	amphibole	Opx	orthopyroxene
An	anortite	Pg	paragonite
Ap	apatite	Prg	pargasite
Arg	aragonite	Phe	phengite
Ath	anthophyllite	Phl	phlogopite
Bar	barroisite	Pl	plagioclase
Bt	biotite	Prp	pyrope
Cal	calcite	Px	pyroxene
Chl	chlorite	Qtz	quartz
Clm	chloromelanite	Rt	rutile
Czo	clinozoisite	Scp	scapolite
Cpx	clinopyroxene	Ser	sericite
Di	diopside	Sil	sillimanite
Ed	edenite	Sps	spessartine
Ep	epidote	Tar	taramite
Fo	forsterite	Ttn	titanite
Fsp	feldspars	Tlc	talc
Grs	grossularite	Ts	tschermakite
Grt	garnet	Tur	tourmaline
Hbl	hornblende	WhM	white mica
Hd	hedenbergite	Zo	zoisite
Ilm	ilmenite	Zr	zircon
Jd	jadeite	WR	whole-rock.

Manuskript bei der Schriftleitung eingelangt am 7. September 1998